VISUALIZATION OF THE FRAGMENTATION OF A WEAK GRANULAR MATERIAL DURING COMPRESSION

by

Carmin Sbarro

BS in Civil Engineering, University of Pittsburgh, 2005

Submitted to the Graduate Faculty of

the School of Engineering in partial fulfillment

of the requirements for the degree of

Master of Science

University of Pittsburgh

2007

UNIVERSITY OF PITTSBURGH

SCHOOL OF ENGINEERING

This thesis was presented

by

Carmin Sbarro

It was defended on

June 4, 2007

and approved by

Jeen-Shang Lin, Associate Professor, Civil and Environmental Engineering Department

Calixto I. Garcia, Research Professor, Materials Science and Engineering Department

Thesis Advisor: Luis E. Vallejo, Professor, Civil and Environmental Engineering Department

VISUALIZATION OF THE FRAGMENTATION OF A WEAK GRANULAR MATERIAL DURING COMPRESSION

Carmin Sbarro, M.S.

University of Pittsburgh, 2007

The purpose of this research was to visualize the crushing of a weak granular material during compression. In order to be able to see the individual particles of the sample with out the usage of sophisticated and expensive equipment, roasted chick peas were used to model granular material. The chick peas were chosen because of their size and availability. A series of uniaxial confined compression tests were run on the chick peas to check different aspects of the fragmentation. All the samples used in the tests were prepared the same way having the same initial height and mass. The samples also had uniform gradation. An initial test was run on the chick peas to an applied vertical load of 3 kN. This test was used to create a void ratio versus the logarithm of the stress curve. From the curve constructed from the results of the first test four applied vertical loads were chosen. These four applied vertical loads were used throughout the research. The first set of uniaxial confined compression tests were used to determine how many chick peas were broken during compression. The next set of uniaxial confined compression tests were used to run sieve analysis on each sample and to determine how the gradation of the sample changed as the applied vertical load increased. Another confined uniaxial compression test was run to a selected load to determine how the crushing occurred internally. Through out the research several pictures were taken with a digital camera to help illustrate the crushing inside and outside the samples. Pictures outside the samples were possible since the cylinders used for the compression tests were transparent. A fractal analysis was done using the results of the sieve

analysis for each sample. Fractal fragmentation dimensions were calculated to determine the degree of crushing at each of the applied vertical loads. Another fractal analysis was done using a Seirpinski Gasket in order visualize the way the samples developed a fractal size distribution. Six level of the gasket were generated and used to model a sample fragmenting during compression.

TABLE OF CONTENTS

LIST OF TABLES

LIST OF FIGURES

PREFACE

I would like to thank Dr. Vallejo from his time, his mentoring, his patience, and most of all his belief in my ability to complete this research project.

I would also like to thank the following people. My parents, Louis and Giorgina Sbarro for being extremely supportive throughout my college career. Patrick Minnaugh for not only answering my annoying questions but also for always being as supportive as my parents. Lisa Abraham and Keith Coogler for making going through graduate school just a little bit more bearable. Sebastian Lobo-Guerrero for being a friend and colleague for his invaluable help in the early stages of my research. Thanks to Dr. A. Koubaa for all the help during my academic career at the University of Pittsburgh. Special thanks also go to Drs. J.S. Lin and C.I. Garcia for serving in the examination committee.

1.0 INTRODUCTION AND LITERATURE REVIEW

1.1 INTRODUCTION

Granular materials are often a component of engineering structures such as earth dams, foundations, pavement bases, and embankments. As a part of these structures, the granular material is subjected to both static and dynamic loading. The loading can result in particle breakage of the granular material. The engineering properties of the material can be negatively altered as a result of the particle breakage, and consequently failure may occur. The behavior of granular material under compression needs to be studied to better understand the occurrence, consequences, and avoidance of particle breakage.

1.2 OBJECTIVE

The purpose of this thesis is to visualize the fragmentation of a weak granular material during compression. This particular research focused on using a weak material which could easily be crushed by standard laboratory equipment. The material used had particles large enough to be seen and identified by the naked eye. Visualization of the behavior during compression could be seen without any use of sophisticated equipment.

1.3 ORGANIZATION OF THESIS

Chapter 1 presents an introduction of the thesis topic. A literature review focusing on research related to the scope of this thesis is included.

Chapter 2 describes the material used to replicate a granular material in the research. A description of the equipment used and the tests on the material are also included.

Chapter 3 focuses on the results of a series of confined uniaxial compression tests run on the material. Included in these results is a void ratio versus the logarithm of time plot for a load of 3kN as well as a sieve analysis for each loading run.

Chapter 4 includes a visualization of where crushing is occurring both internally and externally in the sample. Pictures taken during the confined uniaxial compression test for the 3 kN load are used to show the external crushing. The internal locations are shown by running a confined uniaxial compression test and dividing the sample into equal layers.

Chapter 5 focuses on fractal theory. A brief description of fractal theory is presented. A fragmentation fractal dimension for each of the confined uniaxial compression tests is calculated. An analysis of a Seirpinski Gasket to describe crushing is included as well.

Chapter 6 is the summary and conclusion of the research presented in this thesis.

1.4 LITERATURE REVIEW

1.4.1 Strength and Compressibility

The yield stress is proportional to the grain tensile strength of an aggregate under one-dimensional compression. The current yield stress of an aggregate is determined by the tensile strength of its smallest particles. In turn, this grain strength of a crushable soil also governs the dilatancy and strength of a crushable soil such that dilational component of the internal friction angle is proportional to the logarithm of the mean effective stress when normalized by the tensile strength of the grain(McDowell and Bolton 1998).

Granular soil is very compressible under an applied stress. Compression is usually accompanied by particle crushing. Therefore the two are related to each other

(Lee Farhoomand 1976). The compressibility will depend upon a few key factors such as fractal dimension, particle material toughness, variability in particle tensile strength, and the friction angle of the soil(McDowell et al. 1996). The larger the degree of crushing in a material, the more the void ratio versus the logarithm of time graph will approach linearity (McDowell and Bolton1998). Grain crushing will result in a drop which is marked by a step of the compression curve (Feda 2002), and the existence of linear compression lines. A higher Kc ratio results in a greater degree of particle crushing

(Lee and Farhoomand 1976).

1.4.2 Creep and Time

Creep is accompanied by particle breakage(McDowell and Khan 2003). Creep deformation increases due to the time dependent destruction of the soil grains (Feda 2002).

The larger the amount of particle crushing in a soil, the higher the creep coefficient will become (McDowell and Khan 2003).

The amount of grain crushing will be affected by the time of the loading and the stress path of the material (Feda 2002). Compression and crushing will increase at an "ever decreasing rate" for a given period of time(Lade et al 1996).

1.4.3 Fractal Behavior

A granular material of uniform grain size will break into a new system where its grain size distribution is fractal in nature (McDowell and Bolton l998). The fractal distribution of the system is caused by network of force chains across the material which is also fractal (Vallejo et al 2005).

1.4.4 Factors Influencing Crushing

Uniform soils compress and crush more than a well graded soil with the same maximum grain size (Lee and Farhoomand 1976). More extensive crushing was seen in specimens with a larger median grain size (Hagerty et al 1993).

Angular particles have a higher degree of crushing and compression than rounded particles (Lee and Farhoomand 1976). Angular particles also crush to a higher amount at a lower stresses than rounded particles(Hagerty et al 1993).

The start of particle crushing began at much lower stresses for loose specimens than it did for specimens with denser packing(Hagerty et al 1993).

During the early stages of crushing, the amount of crushing was not uniform through out the sample and concentrated in the upper regions. As the crushing evolved, different sections of the sample tended to reach similar quantities of crushing (Lobo-Guererro et al 2006).

1.5 RECENT RESEARCH ON CRUSHING

1.5.1 Conclusions by Zamri Chik (2004)

Chik (2004) researched “the effect of fragmentation on the engineering properties of granular material” using both laboratory and fractal analysis. Chik first ran a series of tests using the Brohmhead Ring Shear Apparatus on coarse sand, then on three different types of sand in order to compare their results. Chik observed in the beginning stages of the tests on the coarse sand, the readings on the dial were unsteady and cracking was heard during this period. Chik also observed the sand acted as dense sand at low stress but acted as loose sand at high stresses. Chik determined the angle of internal friction decreased with an increase in normal stress and a curved Mohr-Coulomb failure envelope resulted. Chik observed the initially uniform samples became more well graded as normal stress increased. Chik also observed an increase in shear stress, normal stress, and amount of fragments resulted in a large reduction of hydraulic conductivity.

Chik saw the rate of increase of fragments was highest in the early stages but reduced somewhat as time went on. Chik used the test to compare the fragmentation of three types of sand: quarts, Ottawa, and calcareous. Chik chose these particular types of sands because they had very different grain structures. Chik observed there to be different crushing in the sands due to the different amount of fragments produced. Angular quartz sand produced a large amount of fines, sub angular calcareous produced less fines, and rounded Ottawa produced minimal fines. Particle size distribution plots on each of the sands indicated quartz sand exhibited more fractal behavior while the Ottawa and calcareous sand were not as fractal.

Chik ran a series of lab tests to investigate the angle of repose of binary mixtures. Chik used a mixture of quartz sand composed of coarse and fine grains to model a fragmented mixture. Chik used two different bases: smooth glass and porous stone. Chik developed an equation to calculate the angle of repose and used two different methods to physically measure it. From the tests, Chik concluded the angle of repose is relevant in studying fragmentation. Chik observed the influence of interfacial friction between the material and the base in contact has significant influence on the angle of repose. Chik observed in a binary mixture the effect of "basal friction" increases when the resistance is only related to contact area. When there are no interlocking characteristics between the material and base, the angle of repose will be higher. Chik concluded when using a rough surface the angle of repose is a close approximation of the angle of internal friction.

Chik next observed the abrasion of granular materials. Chik tested samples of both round and angular material in the Jar Mill Apparatus. Chik used three different time periods. Chik observed both samples physically showed degradation resulting from abrasion and the surface showed signs of surface attrition. Chik calculated both the Roughness Fractal Dimension and the

Fragmentation Fractal Dimension. Chik observed the angular particles produced a large amount of fines proving the tendency of crushing at the edges and pointed corners of the particles. The sieve analysis showed the angular particles produced approximately four times more fines that the rounded. Chik determined although both types of particles had decreasing Roughness Fractal Dimensions and increasing Fragmentation Fractal Dimensions, the angular particles had more of an increase and decrease. Chik concluded the fragmentation from abrasion is more significant in angular particles than rounded particles under the same conditions.

Chik next researched the effect of crushing on the elastic moduli using the Universal Testing Machine. Chik used three different materials: spherical glass beads, angular gravel, and rounded gravel. Chik observed the glass beads sporadically exploded as compression loads increased causing a sudden decrease of compression. At the maximum load very few explosions occurred. Chik observed a high degree of packing at the top of the cylinder and a lesser degree of packing at the bottom. Chik used initially uniformly sized gravels. Chik observed no explosive crushing but did hear cracking sounds. Chik once again observed total crushing occurred at the top layers close to the piston, and the crushed gravels formed compact layers at the top while the bottom layers were unaffected. Chik observed the angular particles fractured more than the rounded and had more fragmentation migration. Chik concluded the elastic modulus of glass does not indicate an increase in value with respect to an increase in fractal dimension except for when the Versa Loader was at a stress of 500 kPa. Chik concluded both geometries of gravel had almost identical results in terms of fractal dimension. Chik also concluded the elastic moduli tests indicate an increase with the increase in fractal dimension.

Chik concluded his research by studying how fragmentation affects hydraulic conductivity. Chik used both angular and rounded particles. Chik modeled static loading using

the Universal testing Machine, and he modeled dynamic loading by executing a Standard Proctor. Chik observed angular and rounded particles had almost identical particle distribution plots, and only a slight variation between fractal dimensions. Chik determined the fractal dimension to be higher for the dynamic loading than the static which indicates a higher degree of fragmentation. Chik utilized the Constant Head Permeability test to determine the hydraulic conductivity of both geometries at various degrees of fragmentation. Chik concluded the hydraulic conductivity decreased as the Fragmentation Fractal Dimension increased. Chik observed the conductivity decreased significantly more in the rounded particles than in the angular. Chik concluded the angular decreased less since the flow through an angular medium is inefficient in the first place. Chik concluded dynamic loading produces more fragments than static loading.

1.5.2 Conclusions by Kevin P. Hammer (2005)

Hammer (2005) studied the crushing of granular materials under an asphalt pavement due to traffic loadings. For the research, Hammer used field samples obtained from existing roadway base courses and baseline samples were from stockpile locations. Hammer performed a series of laboratory tests and analysis to determine if crushing occurred in the baseline samples.

The results of a grain size distribution curves for each field sample showed that some crushing did occur. Most of the samples contained smaller particles in the lower half of the sample. The crushing was determined to not be severe.

Hammer ran a series of point load tests to study the effects of crushing on the individual particles and to observe the effects of strength on particle size. Each of the samples broke into 2 or 3 pieces. The results of the point load tests indicated there is a decrease in particle tensile

strength with increasing particle size. Hammer ran point load tests on 2 of the samples in both the saturated and dry states. These tests resulted in conflicting results, therefore it cannot be concluded that saturated material crushes easier than dry material from the results of these point load tests.

Hammer tested one baseline sample in the Los Angeles machine to determine if degradation of the sample occurs. Although the material was determined to be a competent and durable material, the testing did show a breakdown and crushing of the particles occurred.

Hammer calculated particle breakage factors and sample permeability from the grain size distributions. The breakage factors ranged from zero to 0.75. Hammer further quantified the crushing of the particles by calculating a Roughness Fractal Dimension using the area-perimeter method. Three of the 4 samples had lower fractal dimensions than baseline indicating some degree of crushing occurred. Hammer also analyzed the degree of crushing by calculating the Fragmentation Fractal Dimension. The Fragmentation Fractal Dimension quantifies the crushing using the sieve analysis. Most of the samples had a dimension close to 2.5 confirming that some degree of crushing has occurred.

1.5.3 Conclusions by Sebastian Lobo-Guerrero (2006)

Lobo-Guerrero (2006) evaluated the crushing in granular materials using the Discrete Element Method, DEM, and fractal theory. Before Lobo-Guerrero simulated the crushing using the computer program, a series of tests were executed using laboratory equipment. Lobo-Guerrero used raw sugar to model a granular media.

The first laboratory test was a confined uniaxial compression test on loosely packed sugar. Lobo-Guerrero concluded the void ratio of the sugar went through three distinct stages. In the first stage, the void ratio changed very little and was considered particle rearrangement. During the second stage, the void ratio went through considerable changes because of crushing of the sugar. The last stage was considered elastic rebound caused by the unloading of the sugar. Lobo-Guerrero ran a sieve analysis on each sample and compared them with the material before loading. Lobo-Guerrero found as the compression levels increased, the percentage of grains with the original grain size decreased while the percentage of grains with a diameter smaller than the original increased. Lobo-Guerrero calculated the Fragmentation Fractal Dimensions using the grain size distributions. The dimensions increased as the applied stress increased, indicating the originally uniform samples became well graded mixtures. Lobo-Guerrero also determined the elastic moduli increased from particle rearrangement and abrasion, but tended to decrease due to particle crushing.

Lobo-Guerrero next ran a series of direct shear tests. Lobo-Guerrero concluded at every vertical stress level, the friction coefficient decreased slightly with displacement. Lobo-Guerrero analyzed the grains of the samples photographically. The analysis showed the samples broke and developed fines with increasing vertical stress and deformation. The photographs showed the sharp corners of the grains broke, and larger grains broke into two pieces. A sieve analysis run by Lobo-Guerrero showed the samples became well graded and achieved the same degree of crushing as reached in the confined uniaxial compression tests. Lobo-Guerrero concluded there is a complex interaction between contraction from crushing and dilatancy from rearrangement.

The final laboratory tests run on the sugar by Lobo-Guerrero were a series of ring shear tests. Lobo-Guerrero found although the mobilized friction coefficient had little variation, the

angle of shearing resistance after was found to be considerably lower than the angle before crushing occurred. Lobo-Guerrero once again determined the originally uniform samples became well graded mixtures. Lobo-Guerrero concluded the amount of crushing in the sample increased as the applied vertical stress increased. Lobo-Guerrero determined the sample reached a stable grading where no further crushing was expected to occur.

The main purpose of Lobo-Guerrero's research was to show the evolution of crushing by simulating the lab tests graphically by DEM. Lobo-Guerrero simulated confined uniaxial compression, direct shear, ring shear, and biaxial compression tests. Lobo-Guerrero concluded from the confined uniaxial tests, crushing of the sample does not occur uniformly but concentrates in different regions. Lobo-Guerrero determined the void ratio for the sample is different in the top of the sample than it is in the bottom.

From the direct shear tests, Lobo-Guerrero concluded the particles in the shear zone transmit larger loads and their coordination numbers became affected by induced displacement, therefore causing crushing to take place at a large vertical stress. Lobo-Guerrero determined the overall porosity of the sample did not change and the compression behavior due to breakage was counteracted by dilation. Lobo-Guerrero also concluded the particle size distributions exhibited a fractal distribution. The peak friction coefficient was reduced because of particle crushing.

Lobo-Guerrero concluded from the ring shear test that sample maintained a constant value of residual friction coefficient despite severe particle degradation. Lobo-Guerrero also determined the particle distribution evolved from a uniform sample to a well graded material that has a fractal distribution.

Lobo-Guerrero concluded from the biaxial compression test the sample exhibited a well defined normal compression line. Lobo-Guerrero saw more crushing occurred during tests with deviator stresses. Lobo-Guerrero once again observed regions where breakage concentrated were different. Lobo-Guerrero determined larger values of stress exhibited a fractal particle size distribution which was dominated by the larger sized original particles and produced more crushing. Lobo-Guerrero also concluded the peak value of internal friction was reduced as a consequence of crushing.

2.0 LABORATORY PROCEDURES

There are two possible ways to research granular material. Testing can be done on stronger material such as rock fragment using sophisticated equipment, or a weak material can be tested using standard laboratory equipment (McDowell and Humphreys 2001).

2.1 USING CHICK PEAS AS GRANULAR MATERIAL.

It has been shown it is possible to use a weak material to with standard equipment to accurately model the behavior of a much stronger material(McDowell and Khan 2003). McDowell and Bolton(2001,2003) used various types of pasta and breakfast cereal to model the behavior of granular material during creep and yielding. Lobo-Guerrero (2006) used sugar to model the behavior of a weak granular material during compression to study if it fragments. This research follows the lead of previous research in using a very weak and relatively easy to find material in place of an actual granular material.

One of the key aspects of the research was to visually see the fragmentation of the material during compression and not just conclude fragmentation has occurred by less direct methods. For it to be possible to see the fragmentation occur, a material large enough for the naked eye to easily see was needed. The material chosen for the research was Chick Peas which are also known as both Garbanzo and Ce Ce beans. The chick peas were chosen to model a

granular material for several reasons. The individual beans were easily seen with out sophisticated equipment. They were uniform in shape and had similar geometry to a real soil particle therefore failing by the same mechanism. The chick peas were very easy to find, and were purchased at the Pennsylvania Macaroni Co. in the Strip District. Most importantly, the chick peas were weak enough to use standard laboratory equipment found in the soils laboratory.

The chick peas were determined to have a specific gravity of 1.399 calculated by measuring the water displaced by a known mass of chick peas. The uniformly sized particles passed through the ½ inch sieve and became caught in the ¼ inch sieve.

2.2 LABORATORY EQUIPMENT.

All laboratory testing was executed in the subbasement of the Benedum Hall of Engineering.

2.2.1 Confined Uniaxial Compression Test

A series of unconfined uniaxial compression tests were conducted on the chick peas with the results used in the various sections. Each test was done in the same way. Each sample was the same mass and height, and as stated before the samples were uniform. The samples were all placed in a Plexiglas cylinder with an internal diameter of 5 cm.

The initial test on the chick peas was run on a Versa Loader machine. A maximum load to take the machine to was dependent upon the limit of the machine. The vertical loads at various points of the confined compression test were determined by using an equation converting

a reading taken from a gage on the machine into a kilo Newton ,kN, load. The equation can be seen below.

$$0.003*(gage\_reading)+0.0189=vertical\_load(kN) \qquad \text{equation 2.1}$$

The figure below shows the versa loader.

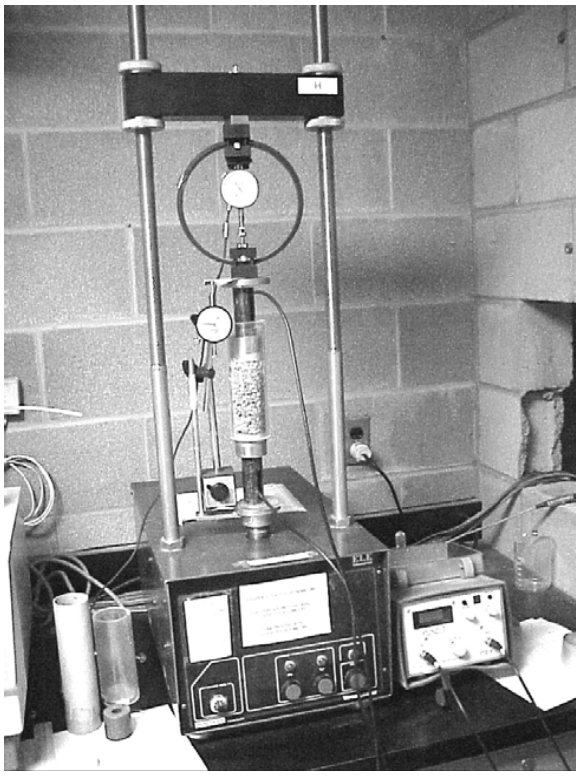

Figure 2-1 Versa Loader machine used in the initial test (Chik 2004).

The remainders of the confined uniaxial compression tests were performed on a machine in the soils laboratory. The machine has a proving ring with a maximum loading of 10,000 pounds. The vertical loads were determined by using an equation relating the deflection of the ring to a reading of the deflection of the ring during loading given during the calibration of the machine. A plot showing a trend line relating the ring deflections to the vertical load as well as the set-up of the machine are shown below.

a)

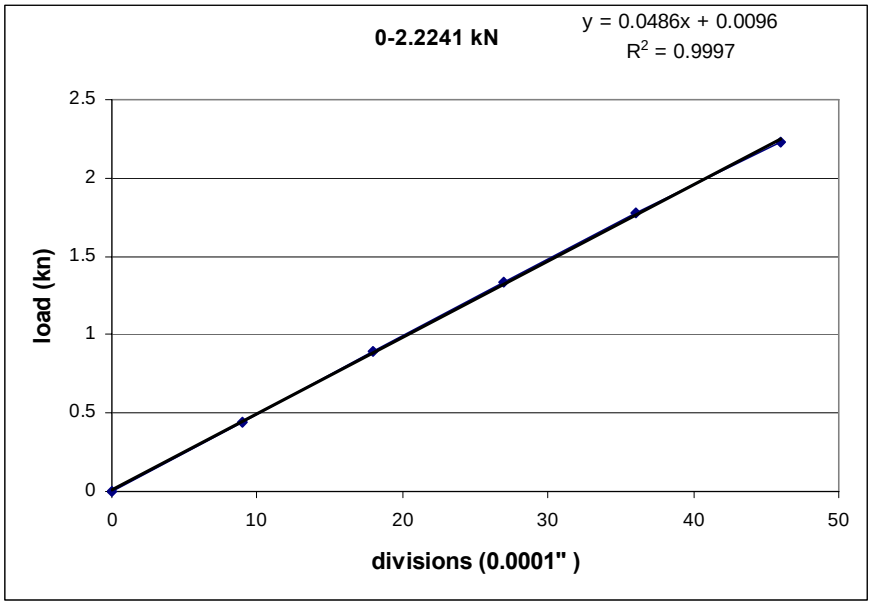

b)

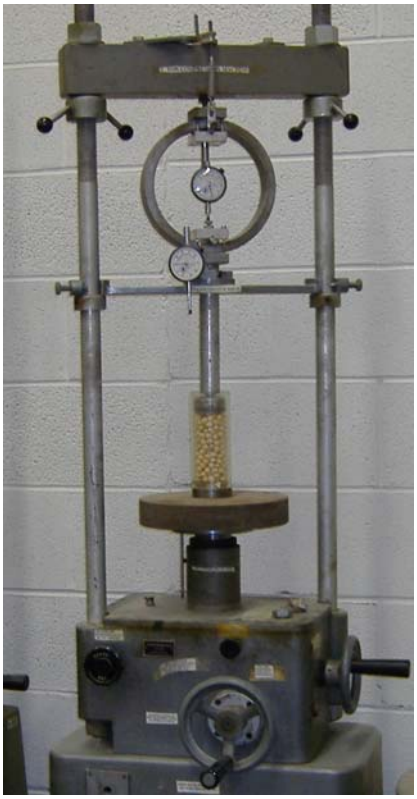

Figure 2-2 (a) Graph created using the ring data (b) Machine set up used to run tests

Each sample was carefully prepared to make sure they had the same height and mass. The initial compression test run set the standard for all the tests which followed.

2.2.2 Sieve Analysis

Since all of the initial samples were uniform, grain size distributions were utilized to illustrate how much crushing occurred. In order to get a grain size distribution, a sieve analysis was run on each of the samples after the tests were completed. The tests were run in accordance with ASTM D 422. A set of six sieves was used: ½ inch, ¼ inch, #4, #10, #20, and #40. Each sample was run on a mechanical shaker for five minutes to distribute the chick peas through the sieves.

The chick peas had a fine powdery coating on them which may have negatively impacted the results of the analysis by creating the illusion more fine material was created. Before the uniaxial confined compression tests were run, the chick peas were placed in the mechanical shaker for approximately ten minutes.

Figure 2-3 Loose materials taken off of the chick peas prior to tests

3.0 LABORATORY TESTING

3.1 CONFINED UNIAXIAL COMPRESSION TESTS

3.1.1 Initial Uniaxial Confined Compression Test

The initial uniaxial confined compression test on the sample was run to a load of 3 kN. As stated in the previous chapter, the limit of the machine was 3 kN, and this is why that stress was chosen. One of the main objectives of the initial test was to create a void ratio versus the logarithm of stress plot. The plot can show many aspects of what is occurring in the sample during compression. One very important feature of the sample behavior taken from the plot is the point of maximum curvature. The point of maximum curvature has been theorized to coincide with the onset of crushing (Hagerty et al 1993).

During the test the deformation of the sample was measured after each complete rotation of the dial gage. Since the deformations were noticeable, a ruler could be used to measure the height of the sample at each gage rotation. The measured heights were used to calculate the void ratios at each stage of stress. The complete table can be seen in Appendix A. Shown below is the resulting plot as well as a table to illustrate how severely the sample deformed during compression.

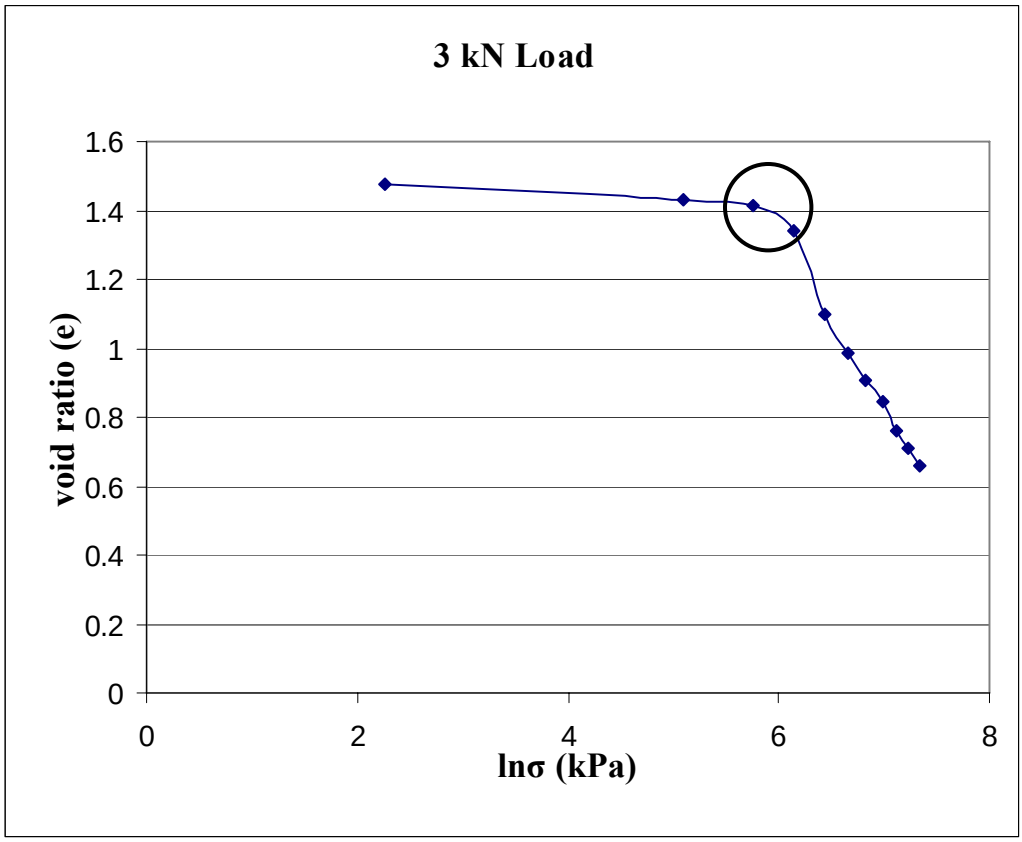

Figure 3-1 Plot of the void ratio vs. the logarithm of the stress for the sample loaded to 3 kN

Table 3-1 Void Ratio Change for the 3 kN Sample

Load (kN)	σ (kPa)	h of sample (cm)	e
0.0189	9.625691	9.8	1.4788135
0.3189	162.41444	9.6	1.4282255
0.6189	315.20318	9.55	1.4155785
0.9189	467.99193	9.25	1.3396964
1.2189	620.78067	8.3	1.0994033
1.5189	773.56942	7.85	0.9855802
1.8189	926.35816	7.55	0.9096982
2.1189	1079.1469	7.3	0.8464631
2.4189	1231.9357	6.95	0.7579341
2.7189	1384.7244	6.75	0.707346
3.0189	1537.5131	6.55	0.656758

The above plot appears to follow the usual trend shown in a granular material during vertical compression stress (McDowell and Bolton 1998). The early stages of vertical compression showed there was very little change in the void ratio changed a very small amount. During the early stages of loading, the chick peas probably went through particle rearrangement. The particle rearrangement would explain why the void ratio had little change. The plot also shows a section where the void ratio changed more significantly than in the beginning. The larger change in void ratio was possibly caused by fragmentation of the chick peas. If the chick peas were severely crushed enough, the smaller particles would probably migrate away from their original space occupied in the sample and fill in the voids between unbroken chick peas. By looking at the plot, the point of maximum curvature appears to be around a vertical load of 1 kN. The point is shown by the black circle on the figure. It can be seen from the table, the height of the sample changed by a very large amount from an initial height of 9.8 cm to a final height of 6.55 cm.

Below is a picture of the sample after the test was completed. The intact chick peas were separated from the crushed chick peas and placed side by side.

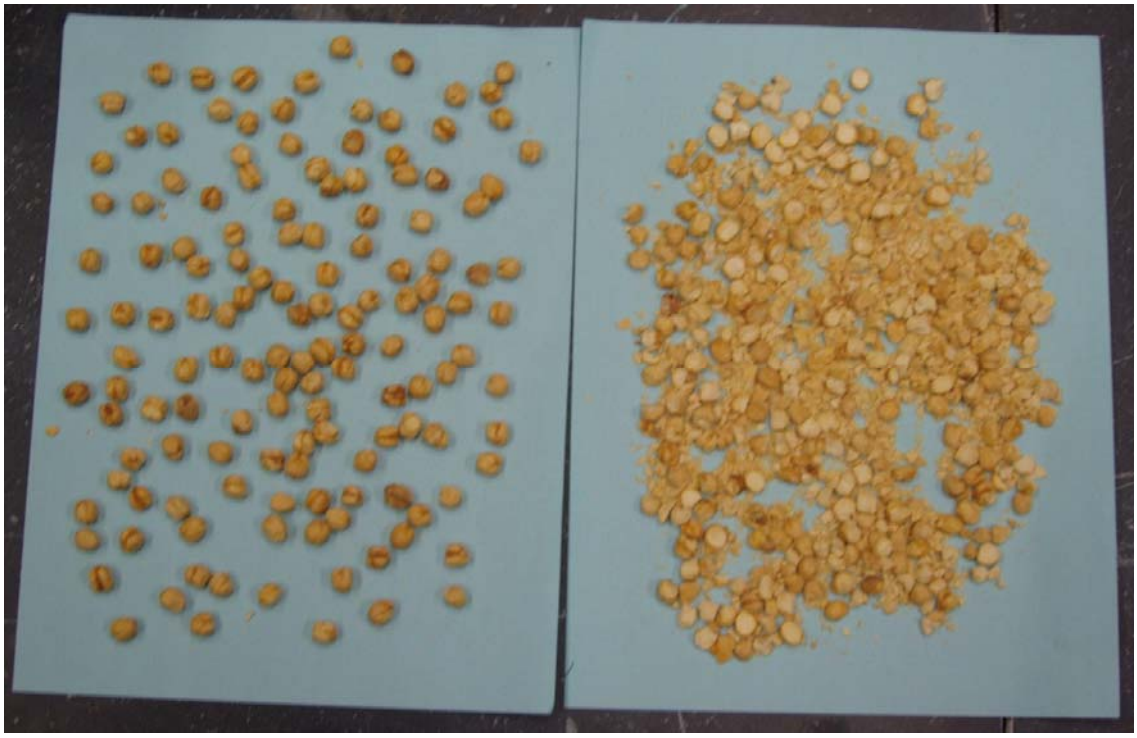

Figure 3-2 Sample after the 3kN test showing the broken and intact chick peas side by side.

From the above figure, it can be seen there is a substantial amount of chick peas that became broken during compression. In fact, it appears as though more chick peas are broken then intact. The broken chick peas were of various sizes which ranged from half to very small and fine.

3.1.2 Further Uniaxial Confined Compression Tests

The initial confined uniaxial compression test yielded a void ratio versus the logarithm of stress plot which followed the trend for a granular material under compression (McDowell and Bolton 1998). From this plot the approximate stress where it reached maximum curvature was found to be at a vertical load of about 1 kN. Four additional vertical loads to execute more uniaxial confined compression tests were chosen based on the approximate vertical load where

the plot exhibited maximum curvature. Two of the vertical loads were smaller than 1 kN, while the other loads were larger. The loads were chosen in this manner to see if fragmentation would occur at the vertical loads before the point of maximum curvature. The additional loads chosen were 0.5 kN, 0.75 kN, 1.5 kN, and 1.75 kN.

The main objective of the further compression tests was to see how many particles in each sample were crushed during the test. Each test was run in the manner described in Chapter 2. The number of chick peas contained in the sample was counted before each test, and then they were counted once the test was complete. In order to compare the results, an average number of particles per sample were calculated from the number of chick peas counted before each test was executed. The average number of particles in a 108.6 g sample was found to be 291. Shown below is a table and chart showing the results of the compression tests.

Table 3-2 Number of Crushed Chick Peas at each Applied Vertical Load

Vertical Load (kN)	# Intact Before	# Intact After	# Crushed Particles	% Crushed
0	291	291	0	0.0%
0.5	291	283	8	2.7%
0.75	291	268	24	8.2%
1.5	291	233	59	20.3%
1.75	291	190	100	34.4%
3	291	140	151	51.9%

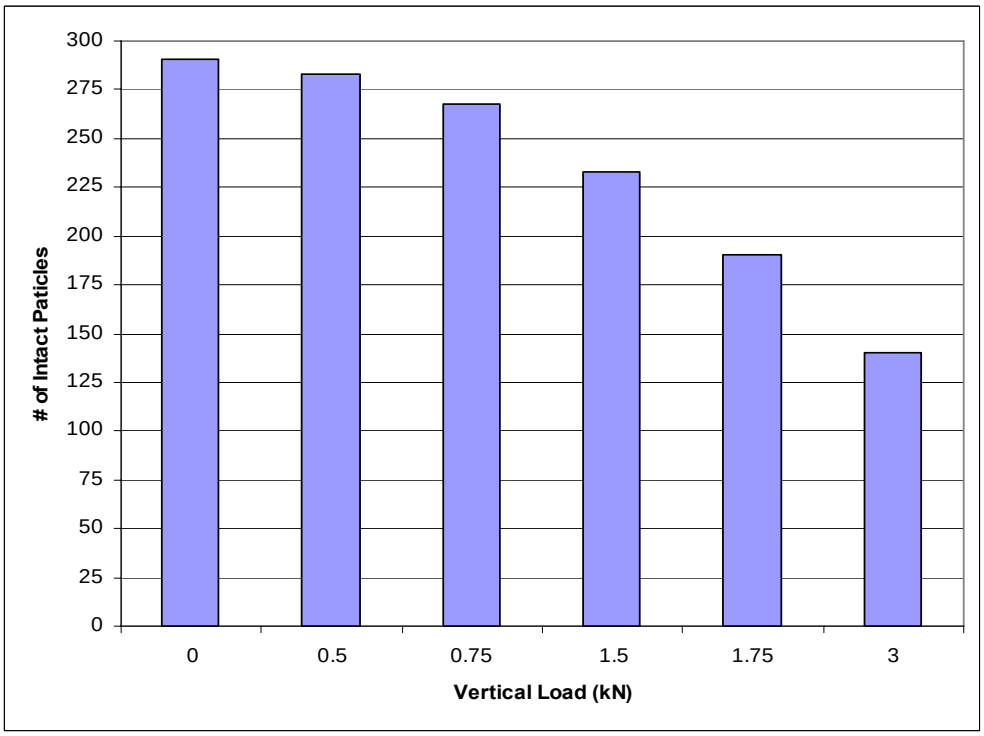

Figure 3-3 Chart showing the number of intact particles after each compression test

The above chart and table also show a number of particles for a vertical loading of 3 kN. The number of intact particles after the test was counted from a photograph taken after the initial uniaxial confined compression test. The number of crushed particles for the 3 kN vertical load was found based on the number intact after the test and the average number of particles calculated at 291 particles.

The chart shows a definite trend in the number of intact particles. As the applied vertical load increases, the number of intact particles decreases. At a vertical load of

3 kN, the bar for the number of intact particles is significantly shorter than the bar for no applied vertical loading.

The corresponding table shows the numerical values for the number of chick peas before, the number of chick peas after, the number of crushed particles, and the percentage of crushed

particle. At the lighter applied vertical loads of 0.5 and 0.75 kN, a small amount of particles are crushed. Only 5 chick peas, 2.7%, were broken during compression. Similarly, at 0.75 kN only 24, 8.2%, were crushed during compression. When the applied vertical load became higher than 1 kN, a larger and more significant number of particles were broken. At 1.5 kN 24 chick peas, 20.3%, were broken, but at a vertical load of 1.75 kN the number of crushed particles increased a great deal to be 100 particles, 34.4%. At the final vertical load of 3 kN, the number of crushed particles was greater than the number of intact chick peas. The number of crushed particles for the 3 kN load was 151 which was 51.9% of the sample.

Another aspect of the further uniaxial compression tests which is noteworthy was the ease at which each of the samples came out of the cylinder after the tests. The samples for applied vertical loadings of 0.5 kN and 0.75 kN came out of the cylinder very easily after the tests. The samples for applied vertical loadings of 1.5 kN, 1.75 kN, and 3 kN did not easily come out of the cylinder. At a vertical load of 1.5 kN approximately half of the sample remained lodged in the cylinder and had to be gently removed with a spoon. At both applied vertical loads of 1.75 kN and 3 kN, the entire sample remained lodged in the cylinder and had to once again be gently removed with a spoon. The cause of the increasing difficulty to remove the sample from the cylinder may be directly related to the vertical deformation of the sample after compression. The change is the height of the sample during compression was shown to be rather significant during the initial uniaxial confined compression test. In the beginning the particles simply rearranged slightly barely causing a decrease in volume, but as the sample began to experience crushing the broken particles may have started to fill in the voids and cause a significant volume change which may have resulted in a “packing” of the sample.

3.2 SIEVE ANALYSIS

A particle size distribution curve resulting from a sieve analysis can show a lot about a sample such as the range of particle sizes to the type of distribution (Das 2002). The different particle sizes found within a sample can also tell many things about that particular sample. This section of the research focuses on the many different items about each of the samples. A sieve analysis was performed on samples on which uniaxial confined compression tests were run on. A separate set of uniaxial compression tests were run than those which were used to find how many particles were crushed. Once again, applied vertical loadings of 0.5 kN, 0.75 kN, 1.5 kN, and 1.75 kN were used for the compression tests. All of the samples were prepared in the same manner keeping a constant height and mass for each of the different samples as well as having a uniform particle distribution.

3.2.1 Particle Size Distribution Curves

Particle size distribution curves, PSD, were created for each of the different samples. The PSD curves for each of the applied vertical stresses were made based on the mass of particles left behind in each of the sieves. A table illustrating the method for one of the vertical loadings can be found in Appendix A. Below is a figure of showing the development of the PSD curves.

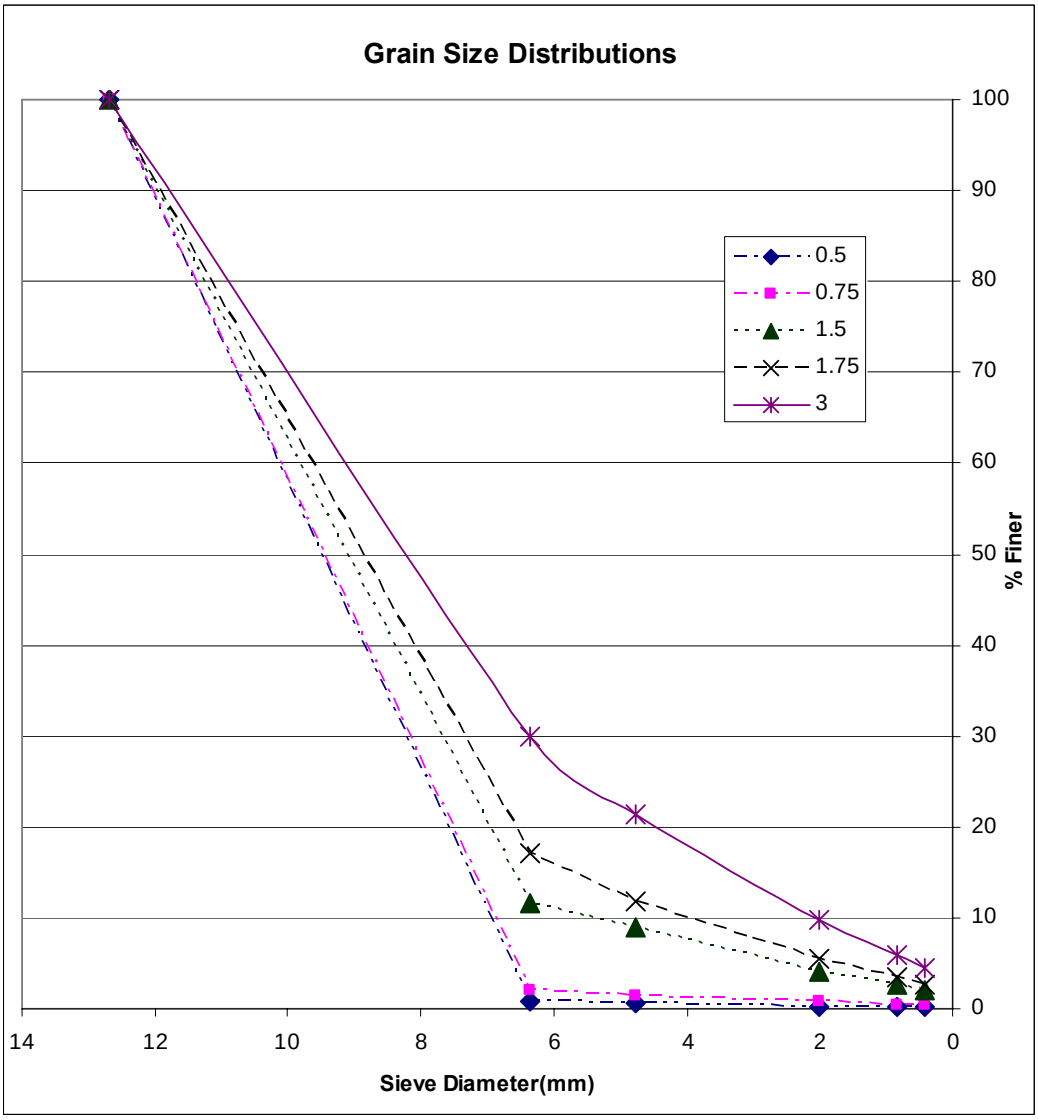

Figure 3-4 The evolution of the PSD plots.

The above figure shows the sample developed from a uniform sample to a well graded sample as the applied vertical stress increased. The PSD curves for the applied vertical loadings of 0.5 kN and 0.75 kN tended toward the shape of a poorly graded sample. The PSD curve for the vertical load of 1.5 kN tended a slight amount toward the shape for a well graded material, but still showed signs of poor grading. The PSD curve for the vertical load of 1.75 kN tended more towards the shape a well graded material, while the PSD curve for the peak vertical load of

3 kN totally tended towards the shaped a well graded material (Das 2002). It is not surprising the lower applied vertical loads had PSD curves tending towards the shape for a poorly graded material since little particle breakage occurred. As the applied vertical load increased the PSD curves tended more towards the shape of a well graded material because the samples lost their original uniformity due to particle breakage.

3.2.2 Effective Grain Size

The effective grain size, D_{10}, is the parameter which corresponds with 10% of the material being finer by weight.. The D_{10} is found directly on the PSD curve and is a good measure to estimate the drainage of water through the soil (Das 2002). Below is a table of the effective grain sizes for each of the applied vertical stresses.

Table 3-3 The Effective Grain Size for Each Load

Load	$D_{10\ (cm)}$
0.5	6.93
0.75	6.07
1.5	5.2
1.75	3.67
3	1.9

It can be seen from the above table the effective grain size decreases significantly as the applied vertical load increased. At the vertical loads of 0.5 kN, 0.75 kN, and

1.5 kN the effective grain size varied only slightly from 6.23 to 5.20 mm, but at a vertical load of 1.75 kN showed a significant drop to 3.67 mm. The peak vertical load of 3 kN had an effective grain size a very large amount smaller than the other loads at 1.90 mm. Once again the

large decline in effective particle size is most probably caused by the particle crushing and the samples becoming well graded.

3.2.3 Coefficient of Gradation

Another parameter that can be calculated by using data directly from the PSD curve is the coefficient of gradation. The coefficient of gradation, Cz, is defined by the following equation.

$$C_z = \frac{D_{30}^2}{D_{60} * D_{10}} \qquad \text{Equation 3.1}$$

D_{30} corresponds to the diameter where 30% of the sample is finer by weight, D_{60} corresponds with the diameter where 60% of the sample is finer by weight, and D_{10} is the effective grain size. A well graded material will have a coefficient of gradation between 1 and 3 for sands and gravels (Das 2002). The coefficient of gradation was calculated for each of the vertical loads and the results are shown in the following table.

Table 3-4 Table of the Coefficients of Gradation for the Loads

Load	D_{10}	D_{30}	D_{60}	C_z
0.5	6.93	8.20	10.13	0.96
0.75	6.07	8.17	10.13	1.09
1.5	5.20	7.67	9.80	1.15
1.75	3.67	7.73	9.67	1.68
3	1.90	6.73	9.03	2.64

In the above table, the values for the coefficient of gradation become larger as the applied vertical load becomes larger also. The samples tested with the vertical loads of 1.75 kN and 3 kN are the most graded, the latter having a coefficient very close to 3.

3.2.4 Breakage Factor

As explained before the effective grain size, D_{10}, is a valuable parameter. Lade et al(1996) proposed a breakage factor based upon the effective grain size of the initial sample, D_{10i}, and the effective grain size of the final sample, D_{10f}. The breakage factor is shown in the following equation.

$$B_{10} = 1 - \frac{D_{10f}}{D_{10i}} \qquad \text{Equation 3.2}$$

A value of 0 constitutes no particle breakage while a value of 1 constitutes infinite breakage. The value for the initial effective grain size was taken as 12.7 mm since the sample was uniform initially. A calculation to find the breakage factors for each of the samples was done and the results are shown in the following table.

Table 3-5 Table of the Breakage Factors for Each Load

Load	D_{10}	D_{30}	D_{60}	Cz
0.5	6.93	8.2	10.13	0.9578225
0.75	6.07	8.17	10.13	1.0855404
1.5	5.2	7.67	9.8	1.1544133
1.75	3.67	7.73	9.67	1.6837067
3	1.9	6.73	9.03	2.6399079

From the preceding table it can be seen the values of the breakage factor increase as the vertical load increases. The factors for the applied vertical loads of 0.5 kN,

0.75 kN, and 1.5 kN are relatively close to 0 and show that a significant amount of breakage did not occur. the breakage factors for the vertical loads of 1.75 kN and 3 kN are higher and show the sample did have a significant amount of particle breakage. Since the breakage factor for the peak vertical load of 3 kN was only 0.85, it may be concluded the chick

peas have not reached being totally crushed and more fragmentation may occur at loads higher than the peak vertical load.

3.2.5 Permeability

How water flows through a soil is very important in the study of soil mechanics. A soil is permeable because interconnected voids which water can flow through exist within it. One measure of the permeability of a soil is its coefficient of permeability, k. The coefficient of permeability varies widely for different types of soil and depends on factors such as the grain size distribution and void ratio (Das 2002). The effective grain size taken from the PSD curve can be used to calculate k. Hazen (1911) proposed the popular correlation between the effective grain size and k shown in the following equation.

$$k = 100 * D_{10} \qquad \text{Equation 3.3}$$

In the preceding equation, k is the coefficient of permeability in cm/sec and D_{10} is the effective grain size in cm. The coefficient of permeability was calculated for each of the samples as well as the original uniformly graded sample. A table of the results of the calculation is shown in the following table.

Table 3-6 Table of the Permeability for Each Load

Load (kN)	D_{10} (cm)	k(cm/sec)
original	1.27	161.29
0.5	0.69	48.02
0.75	0.60	35.50
1.5	0.52	27.04
1.75	0.37	13.47
3	0.19	3.61

The results in the preceding table show a decrease in the permeability coefficient as the applied vertical stress increases. The coefficient of permeability calculated for the original uniform sample is the largest. The coefficient of permeability decreased significantly as the effective grain size for each of the samples decreased. The coefficient of permeability was low for the applied vertical loads of 1.75 kN, and for the peak vertical load of 3 kN the coefficient was extremely low. The particle breakage which occurred during compression significantly decreased the permeability of the samples. the large decrease in permeability may be caused by a decrease in the amount of interconnected void spaces due to both the filling up of void spaces by smaller particles which migrated during compression and by the deformation of the sample.

3.3 SUMMARY

The purpose of this chapter was to see how much crushing occurred in the chick peas using laboratory testing. A test to an applied vertical load of 3 kN was run initially. This initial test showed the chick peas did indeed follow the trend of a granular material based on the void ratio versus the logarithm of stress curve. The sample went through a large amount of deformation and extensive fragmentation. Four other applied vertical loadings were chosen to run uniaxial confined compression tests on based on point of maximum curvature of the aforementioned graph having two before the point and two after the point. These stresses were 0.5 kN, 0.75kN, 1.5kN, and 1.75 kN. A count of the intact particles was done before and after each test. As the applied vertical load increased so did the amount of crushed particles.

Another set of uniaxial confined compression tests was run using the same applied vertical loads as before. The second set of tests was used to construct PSD curves. As the

applied vertical loads increased so did the gradation of the samples. The sample done at the highest applied vertical load of 3 kN tended very much toward the shape of a well graded sample while the samples at 0.5 kN and 0.75 kN were still very uniform in size.

The effective grain size as well as the values for D_{30} and D_{60} was found using the PSD curves. The effective grain size decreased drastically as the applied vertical load increased. Several factors were calculated using the different grain sizes found from the PSD curves: the coefficient of gradation, a breakage factor, and the permeability. As the applied vertical load increased so did the breakage factor, but the permeability decreased a large amount. The laboratory analysis showed the chick peas underwent a large amount of crushing which drastically changed the make-up of the sample.

4.0 THE VISUAL EVOLUTION OF CRUSHING

It has been stated in previous chapters one of the main reasons for using the chick peas was because they are large enough for the naked eye to see. This chapter will mainly focus on visually seeing the evolution of crushing. The evolution will be studied in two ways: internally and externally.

4.1 EXTERNAL EVOLUTION

Earlier research by Lobo-Guerrero (2006) showed crushing began in the upper layers and was not an isolated event in the beginning. As crushing progressed, all regions of the sample seemed to have crushing. To show the external crushing, photographs taken during the initial confined uniaxial test to a peak applied vertical loading of 3 kN were closely analyzed. The photographs were all taken from the same side of the sample as the test was going on. Unfortunately not all of the photographs could be used since not all of them came out clearly. Each of the pictures was inspected to see where crushed particles occurred at the periods of different stresses during the compression test. Once an area where there appeared to be crushed chick peas was discovered, a dark dot was placed over that are in the photograph. A figure was constructed using the photographs marked for crushed particles and the void ratio versus the logarithm of stress plot made for Chapter 3. The figure is shown below.

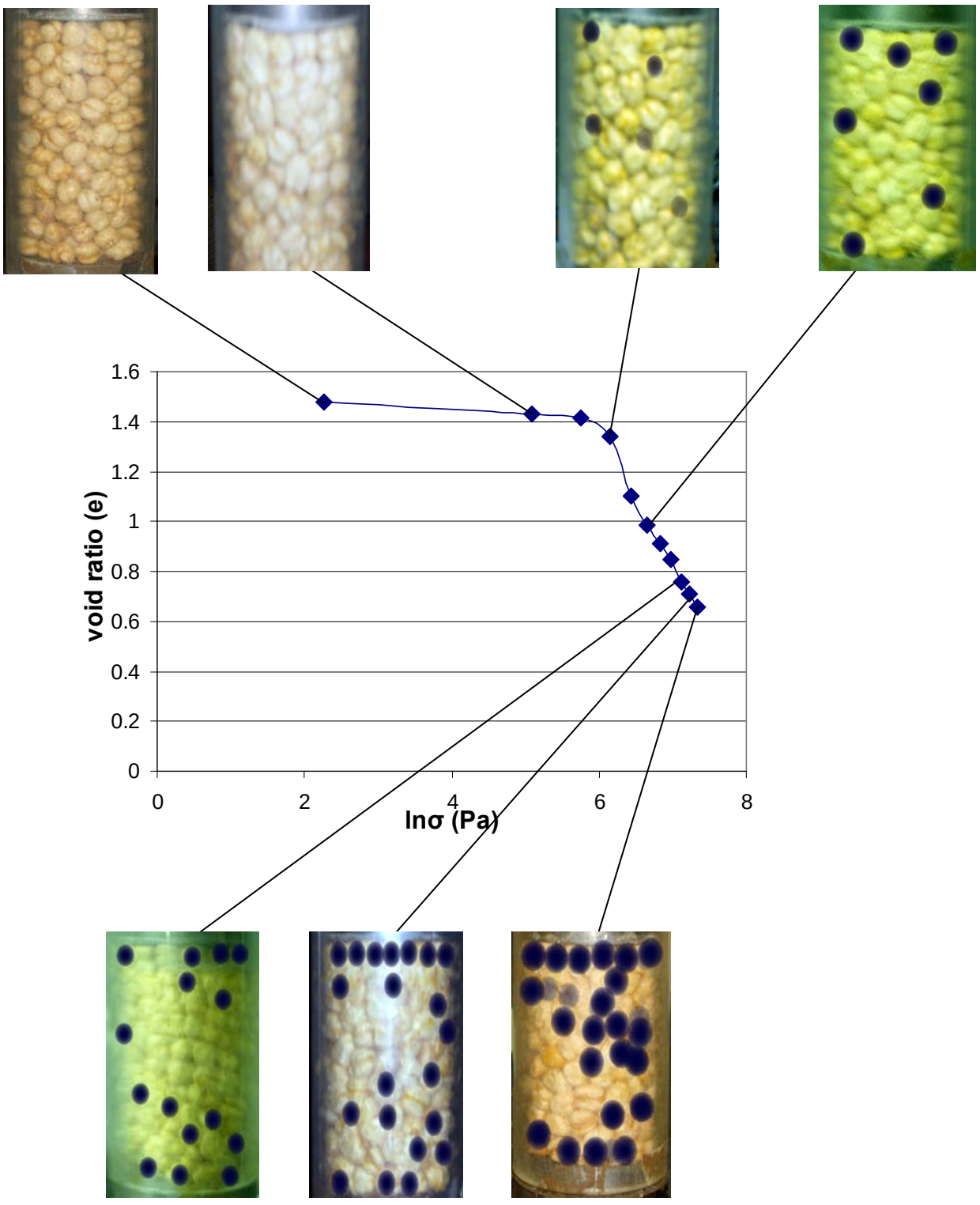

Figure 4-1 External Evolution of crushing on one side of the 3 kN sample

It can be seen from the above figure, no crushing was seen during the early stresses. Sections of crushed chick peas were seen to occur after the section of the plot where maximum curvature occurs. The crushing appears to have begun at the top region of the sample. As the test progressed, crushing was seen in the middle and bottom regions of the sample. The first two pictures where crushing occurred did not appear to have a significant amount of particle breakage, this corresponds with earlier findings for an applied vertical load of 1.5 kN where crushing did occur but not enough to significantly change the gradation of the sample. The pictured of the sample at higher levels of stress appeared to have more areas where crushing occurred, and at the peak level of stress a substantial amount of the sample is covered with regions where crushed chick peas were seen.

4.2 INTERNAL CRUSHING

The evolution of crushing does not just occur externally. The next objective of the research was to see what happens inside the sample during compression.

4.2.1 Method

On order to internally show what happened in the sample, an applied vertical load was chosen based on the yield stress as defined by the point of maximum curvature on the void ratio versus the logarithm of stress graph. Once the applied vertical stress was chosen yet another uniaxial confined compression test was run at this load. The chosen applied vertical load was 1.5 kN. The load was chosen for multiple reasons. First, the load fell after the load where it had

been theorized crushing occurs and the crushing in the sample was seen previously at this load. Another reason, the most important reason, was at this applied vertical load previous tests on the sample did not result in the sample becoming so deformed it was tightly packed in the cylinder upon completion of the test.

A total of two tests were run on two separate samples. The uniaxial confined compression tests were run on the same manner as described in Chapter 2. Each of the samples had the same height and mass. Upon completion of the test, the sample was measured then divided into layers of equal thickness. The layers were marked on the outside of the cylinder with a marker. Each test resulted in an final height of 8 cm, and the sample was separated into eight layers. The layers were numbered in descending order from the top. Each layer was carefully removed from the cylinder with a plastic spoon and placed separately. The method of separating the samples made it important for the sample to not be too cemented together after completion of the test. Photographs were taken at the top of each layer while in the cylinder, and photographs were also taken of the separated layers once removed from the cylinder.

4.2.2 Internal Results

In order to fully illustrate the internal behavior of the sample, several pictures were taken. A series of photographs were taken directly above each layer before it was removed from the cylinder. Another series of photographs were taken once each layer was removed from the cylinder.

4.2.2.1 Aerial View of Sample

The following figure shows the top of each individual layer while it is still in the cylinder.

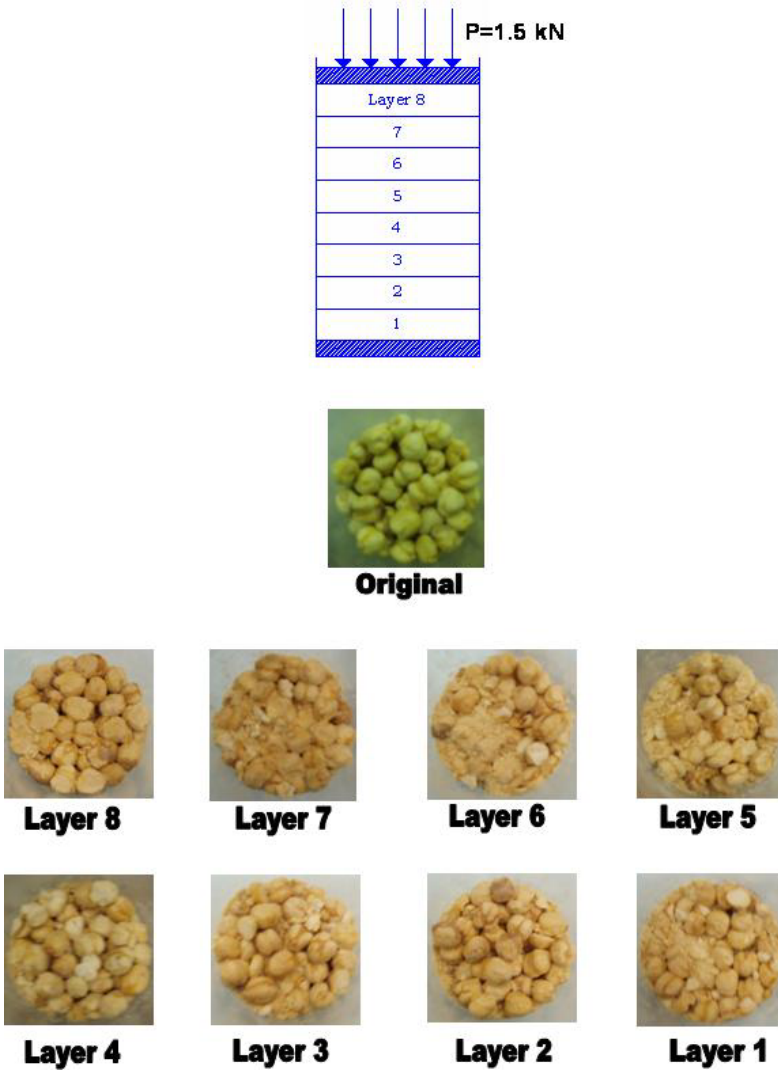

Figure 4-2 Aerial views of the tops of each layer

The preceding figure also shows the top of the sample before the test was executed. Layer 8 was the layer directly below the piston. It has the most noticeable damage to the individual chick peas. There are several crushed chick peas and a number of chick peas which appear to be "flattened." There is no presence of fine material at the top of the 8th layer. Layer 7

also has a number of chick peas which are broken. The top of the layer has a small amount of fine material. Layer 6 has a large amount of fine material present at the top. The layer also yields a few broken chick peas. Layer 5 has a small amount of fines at the top. The layer also has a few broken beans, but not as many as in layers above it. Like layer 5, layer 4 only has a few broken chick peas and a very small amount of fine material is present. Layer 3 has a little fine material, but a large amount of broken chick peas. Layer 2 has very little fine material, much less than the layers above it. Layer 2 has some crushed chick peas. The bottom layer, layer 1, has a large amount of fines and some crushed chick peas.

4.2.2.2 Layers Outside of the Cylinder

A figure showing the photographs of the layers once they have been taken out of the cylinder is shown below.

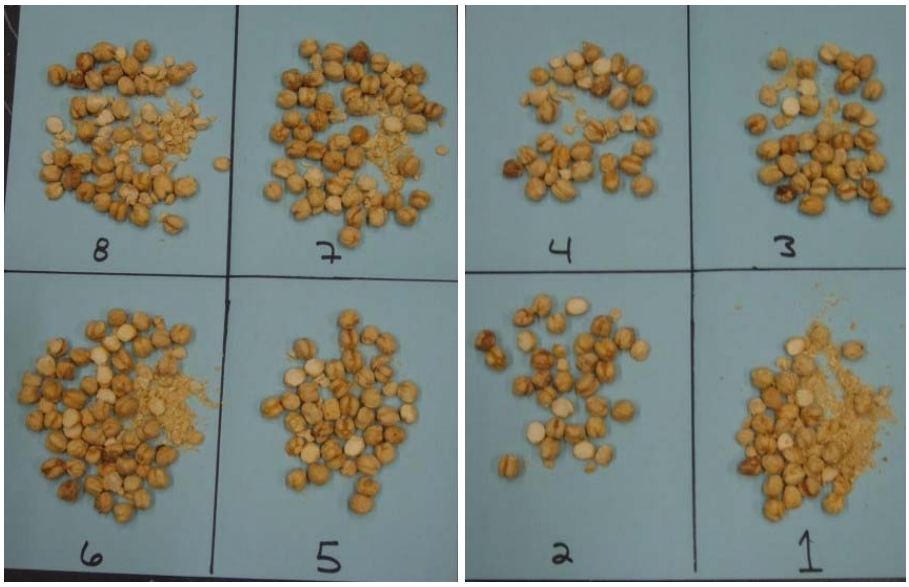

Figure 4-3 Chick peas from each layer of the sample taken out of the cylinder

It can be seen from the preceding figure fine material is found in very distinct areas of the sample. The layers closest to the piston have fine material present in them. The middle layers do not have any fine material present in them. The bottom not only has fine material present, but it has the largest concentration of fine material. The photographs also show the layers closest to the piston have more particles than the middle and bottom layers. The figure also shows the broken chick peas are not evenly distributed through out the sample. Although broken chick peas are present in most of the layers, the amount in each layer is not the same. The layers at the top of the sample exhibit the most particle breakage. The middle layers appear to have the least amount of breakage present.

4.2.2.3 Conclusions from the Internal evolution

After seeing two different views of the layers internally, some conclusions can be made. The top of the sample and the bottom of the sample appear to have different void ratios. Lobo-Guerrero (2006) also found a similar result in his evaluation of a confined uniaxial compression test. The top of the sample would have a void ratio less than the bottom of the sample. The smaller void ratio would account for the upper layers having more chick peas than the bottom layers. The smaller void ratio would also explain why the fine material was trapped in the upper layers and then why a large amount of fine material was present in the bottommost layer, layer 1.

4.3 SUMMARY

The purpose of this chapter was to get a visual understanding of how the crushing in a sample develops. Pictures taken during the uniaxial confined compression test to an applied vertical loading of 3 kN were used for an external evaluation. The pictures showed the crushing did not begin until after the point of maximum curvature on the graph. The crushing also began in the section closer to the piston, which could be due to friction. As the stress increased so did the amount of crushing. After the top region, it appeared the bottom region began to experience crushing, but as the test progressed and the maximum stress was accomplished crushing was seen in all regions of the sample.

The next way the crushing was visualized was internally by separating out equal layers of a sample. An applied vertical load of 1.5 kN was used, because the sample easily came out of the cylinder at this level of loading. Eight layers of equal heights were used. The internal investigation showed the layers closest to the piston, layer 8 to layer 6, not only experienced more crushing, but also had more chick peas contained in them. The layers closer to the middle and bottom of the sample, layer 5 to layer 1, had very few broken chick peas and were not packed as tightly as the top three layers. The amount of fines found in each layers was also no equal. Layers 8 through 6 had fines in them but layers 5 through 2 did not. Layer 1 had a very large amount of fines within its chick peas. The sample appeared to have different void ratios from the top to the bottom. The top of the sample was packed much tighter and was able to trap fines. The middle and bottom of the sample had a much looser construction which allowed the fines to fall though to the bottom layer.

5.0 FRACTAL ANALYSIS

In Euclidean geometry the dimension of geometric shapes is an integer. A point is zero dimensional, a line is one dimensional, a plane is two dimensional, and a sphere is three dimensional. In nature “shapes” are not so easily characterized by integer dimensions. Even the Earth itself is not a totally smooth sphere. In that case, the dimension may not be best described by an integer value, and it may in fact have a fractional dimension. The research for this thesis studied two types of fractal dimensions: the Fragmentation Fractal Dimension as found by the method of Tyler and Wheatcraft(1992) and a fractal dimension as established by using a Seirpinski Gasket.

5.1 WHAT IS A FRACTAL?

B.B. Mandelbrot (1982) concluded many patterns in nature are too irregular and fragmented and have a higher degree and more complexity than can be described by Euclidean Geometry. He developed a new type of geometry solely for nature and used it for a diverse number of fields. The fractal dimension describes the irregular patterns around us and had led to many full fledged theories. Most of the useful fractals involve chance are statistical. Fractal shapes also tend to be “scaling” which implies the degree of irregularity and/or fragmentation is identical at all scales (Mandelbrot 1982). Mandelbrot ultimately described a fractal as “ a shape

made of parts similar to the whole in some way." A fractal looks the same way no matter what the scale is (Feder 1988).

5.2 FRAGMENTATION FRACTAL DIMENSION

5.2.1 Theory

During erosion rock degrades or fragments into soil in a way that appears to be complex and random. It is logical to assume fractal dimensioning can be used to quantify size distribution (Vallejo and Hyslip 1997). Tyler and Wheatcraft(1992) developed a way to use the sieve analysis to find the Fragmentation Fractal Dimension, D_F. Their method uses the mass retained in a sieve and its corresponding diameter. The following equations are used in the process.

$$\frac{M(R<r))}{M_T} = \left(\frac{r}{r_L}\right)^{3-D_F} \qquad \text{equation 5.1}$$

where M(R<r) is the cumulative mass of particles with R size smaller than the given comparative size r; M_T is the total mass of particles; r is the sieve size opening; r_L is the maximum particle size defined by the largest sieve size opening; and D_F is the fragmentation fractal dimension. The dimension is found by using the following equation

$$D_F = 3 - m \qquad \text{equation 5.2}$$

where m is the power of the right hand side of Equation 5.2

Turcotte (1997) determined D_F to be 2.5 if pure crushing has occurred by analyzing the results of several tests on different materials, and ultimately discovered this dimension by testing ice.

5.2.2 Procedure

A separate set of unconfined uniaxial compression tests was run on the chick peas. Once again the vertical loads used were 0.5 kN, 0.75 kN, 1.5 kN, 1.75kN, and 3 kN. Each sample was prepared in the same manner as previous tests having the same mass and height. After each test, a sieve analysis was run using the method as described in Chapter 2. The weight retained in the sieves was used for the Fragmentation Fractal Dimension analysis as described by Tyler and Wheatcraft (1997). An example of the calculation for one load can be found in Appendix C. Below in Fig. 5.1 is shown a representation of Equations 5.1 and 5.2 that it is used for the calculations of the Fragmentation Fractal Dimension, D_F. For example when the uniaxial compressive load was equal to 0.5 kN, m was equal to 1,3571, Thus, the Fragmentation Fractal Dimension D_F was equal to 1.5581 (3-1.4419). When the uniaxial compressive load was equal to 0.75 kN, D_F = 1.6429 (3-1.3571). When the uniaxial compressive load was equal to 1.5 kN, D_F = 2.0051 (3 – 0.9949). When the uniaxial compressive load was equal to 1.75 kN, D_F = 2.0324. And when the uniaxial compressive force was equal to 3 kN, the D_F = 2.1293. Thus, as the fragmentation of the samples increased as a result of larger compressive loads, the fractal dimension also increased.

a)

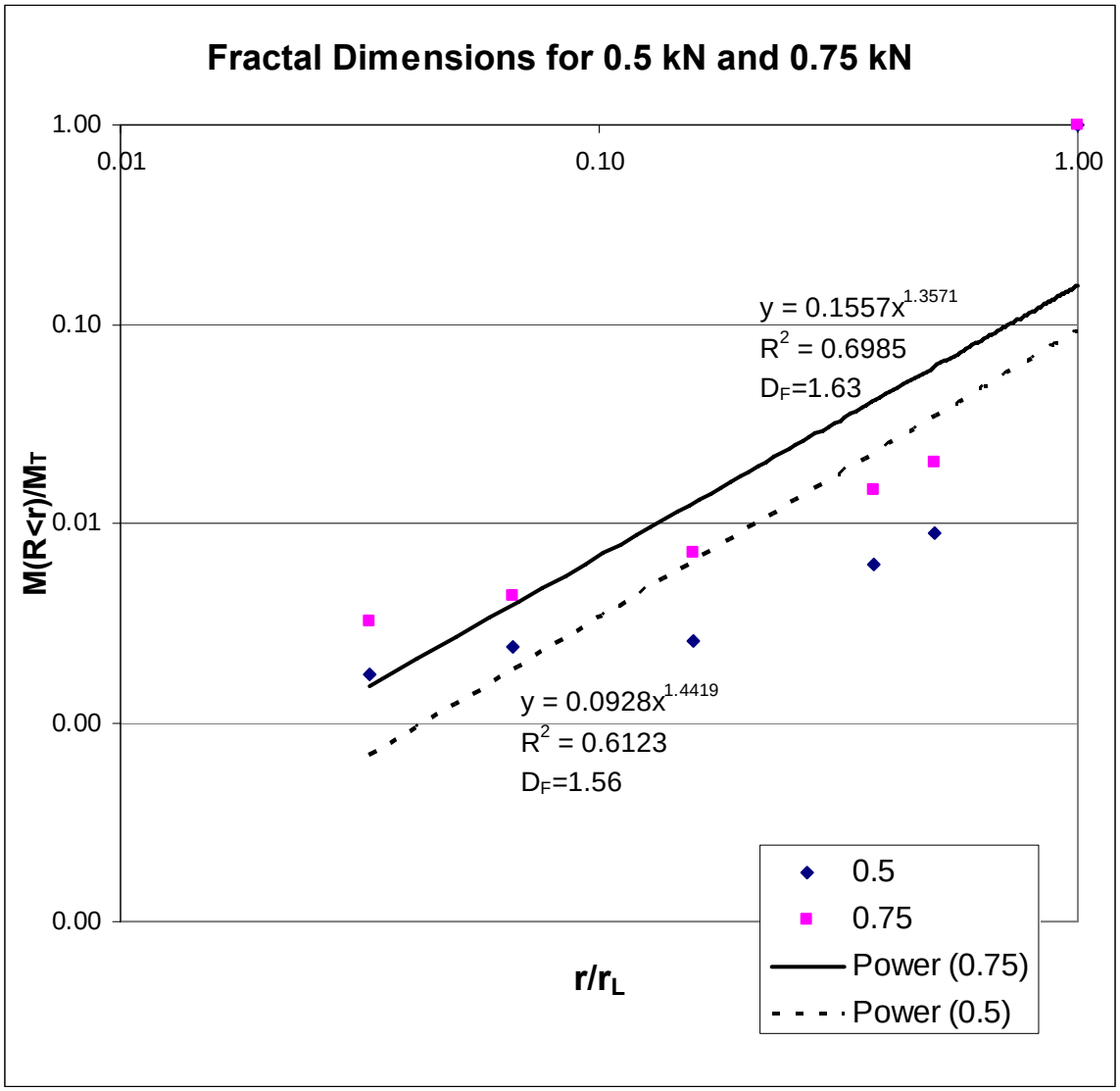
Fractal Dimensions for 0.5 kN and 0.75 kN
1.00
0.01
0.10
1.00
0.10
0.01
0.00
0.00
M(R<r)/MT
y = 0.1557x1.3571
R2 = 0.6985
DF=1.63
y = 0.0928x1.4419
R2 = 0.6123
DF=1.56
0.5
0.75
Power (0.75)
Power (0.5)
r/rL

b)

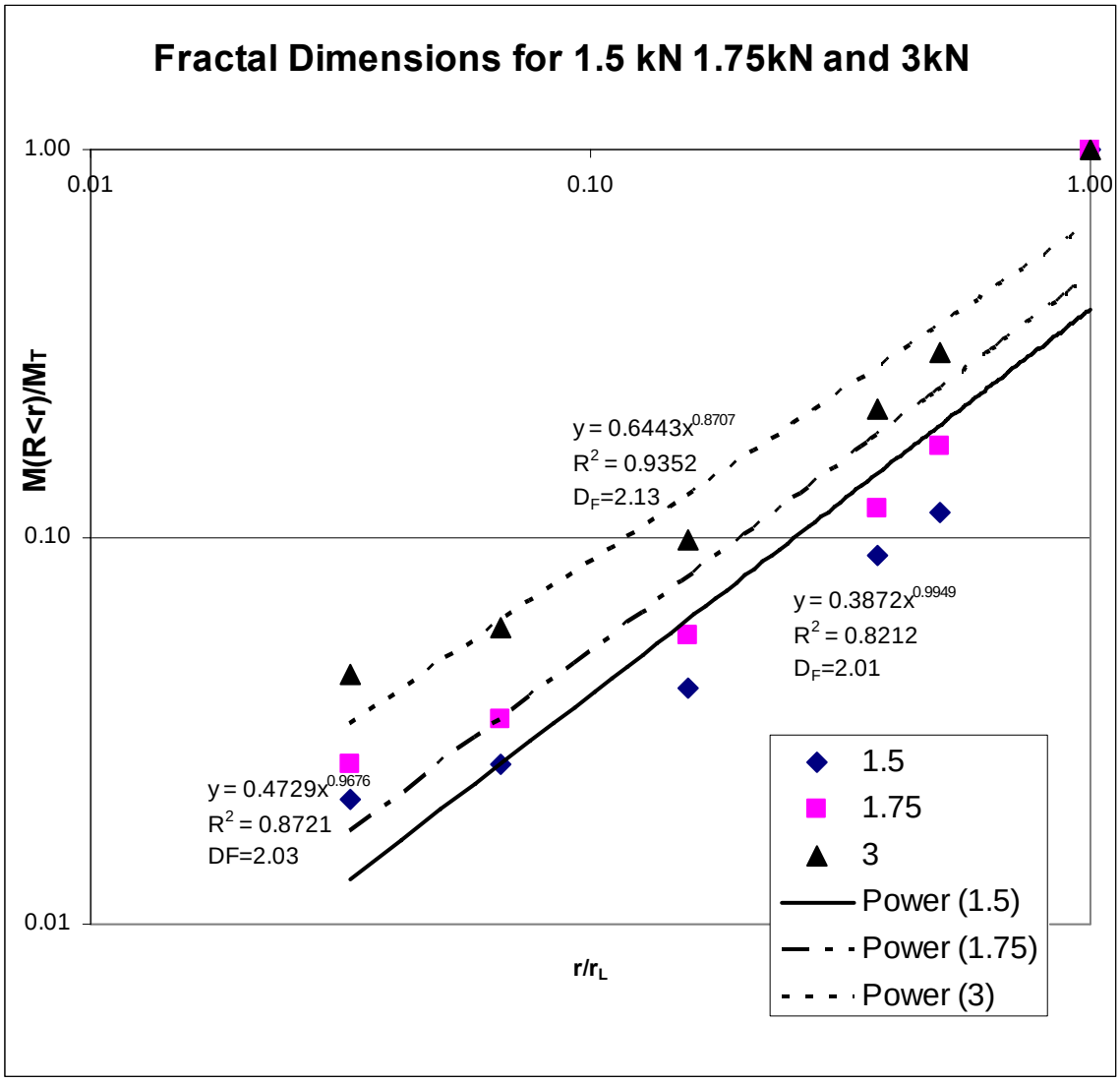

Figure 5-1 (a) Graph for 0.5 & 0.75 kN loads (b) Graph for 1.5, 1.75,& 3 kN loads

5.2.3 Results

It can be seen from the above figures the D_F increases as the applied vertical load increases. The results were separated into 2 separate figures to illustrate how little fragmentation occurred during the applied vertical loads of 0.5 kN and 0.75 kN. At these lighter loads the R^2 values for the trend line are not close to a value of 1 showing very little correspondence to the actual data. For the higher applied vertical loads of 1.5 kN, 1.75 kN, and 3 kN the R^2 values are much closer to a value of 1 showing a much better correlation between the trend line and the actual data.

The results show little fragmentation occurred during the tests when the applied vertical load was less than the yield stress, 0.5 kN and 0.75 kN. In these samples, the larger particles still dominated the behavior of the sample. As the applied vertical load became larger, there was also an increase in the fragmentation as shown by the increasing $D_{F.}$ At the highest applied vertical load, 3 kN, the DF is 2.1293. According the Turcotte (1997) a sample has reached total crushing when the fractal dimension is 2.5. The D_F value of 2.13 at the applied vertical load of 3 kN shows the beans have not been "totally crushed," even though at this level of loading the sample went through a significant amount of crushing that produced a set of particles of different sizes.

5.3 SEIRPINSKI GASKET

5.3.1 Theory

The Seirpinski gasket is a construction which uses an area enclosed by equilateral triangles. This area is divided into a set of larger and smaller triangles each having different area values. In the first generation, the larger triangle is divided into 4 triangles of the same area. In the second generation, one of the four triangles (the one in the center) is left without dividing, and the other three triangles surrounding this central triangle are divided into four smaller triangles of the same area. In the third generation, the central triangle of the four triangles is left without dividing, however the three triangles surrounding this triangle is divided into four smaller triangles. Fig. 5.2 (a) represents this third generation of generating triangles from the original single equilateral triangle. Fig. 5.2 b represents the fourth generation; fig. 5.2 c represents the fifth generation and so on. What this division of the triangle represents is the grain size distribution (in this case the distribution of areas) that is fractal in nature. The number of areas greater than a certain size are counted and used to calculate the Fragmentation fractal dimension using Equation 5. 3 below For this research the different areas that an equilateral triangle can be divided was used to model a sample undergoing fragmentation during compression. The equations used to define the fractal dimensions measured the fragmentation through the size-number relationship of the population of different areas within the gasket (Vallejo and Hyslip 1997). The following equations were used to find the fractal dimension.

$$N(A > a) = ka^{-D/2} \qquad \text{equation 5.3}$$

$$\log N = \log k + \frac{D}{2}\log a \qquad \text{equation 5.4}$$

$$D = -2m \qquad \text{equation 5.5}$$

where N(A>a) is the total number of triangles with the area "A" which is greater than a comparative area "a"; and k is a proportionality constant. where m is the power of the right hand side of Equation 5.3.

5.3.2 Procedure

The different levels of the Seirpinski gasket used in this part of the research were generated using AutoCAD 2005. The first level was an equilateral triangle with sides with a length equal to 20 units. The initial length of the side was chosen arbitrarily mainly for ease of construction. Six levels of division of the area of an equilateral triangle were generated in order to calculate the Fragmentation Fractal Dimension with the help of Equations 5.3 to 5.5. Only six levels were used because at this level, the area of the smallest triangles became extremely small. The very small areas were difficult to see and measure. An attempt was made to generate a 7^{th} level but was stopped due to the previous reasons.

The areas for each of the different sized triangles were obtained using the "area" command with in the AutoCAD program. The dimensions for each level were obtained using Excel and an example of the calculation can be found in Appendix B. Since the gasket used was two dimensional, a value of 1 needs to be added to apply the procedure to a three dimensional application.

5.3.3 Why use the Seirpinski Gasket?

The gasket was used as a model for fragmentation of a sample. Each successive level of area divisions of the triangle represents what happens to a granular sample when subjected to crushing. As the level of axial compression increases. The Seirpinski gasket that uses the equilateral triangle is a viable option to describe the fragmentation of a homogeneous sample for various reasons. The first reason being the fractal dimension resulting from an infinite number of generations is 1.58 (Feder 1988). Adding a value of 1 to the fractal dimension of the two dimensional gasket gives a fractal dimension of 2.58 for a three dimensional application. According to Turcotte (1997) the fractal dimension for a totally crushed specimen is 2.5. The two fractal dimensions for the infinite generated state of the gasket and the fractal dimension for a totally crushed sample are very close to each other in value.

Another reason the gasket works well modeling the phenomenon of crushing is in the way each successive level is generated. When constructing the gasket, one replaces certain triangles with four equilateral triangles. In a group of four triangles the triangle in the middle does not get replaced with the equilateral triangles. During fragmentation, it is theorized the amount of particles surrounding a given particle will dictate if the particle breaks. A particle which is surrounded by many particles is less likely to fragment. This behavior is similar to the construction of the gasket and therefore shows it to be an adequate model for fragmentation. The successive replacement of triangles of a certain area with triangles of a lesser area also mimics the behavior of a uniform sample becoming well graded.

5.3.4 Results

Using equations 5.3 through 5.5 the fractal dimensions for level three through level six were calculated. An example of the calculation can be found in Appendix C. In the figure below are the different levels of the gasket with their corresponding fractal dimension.

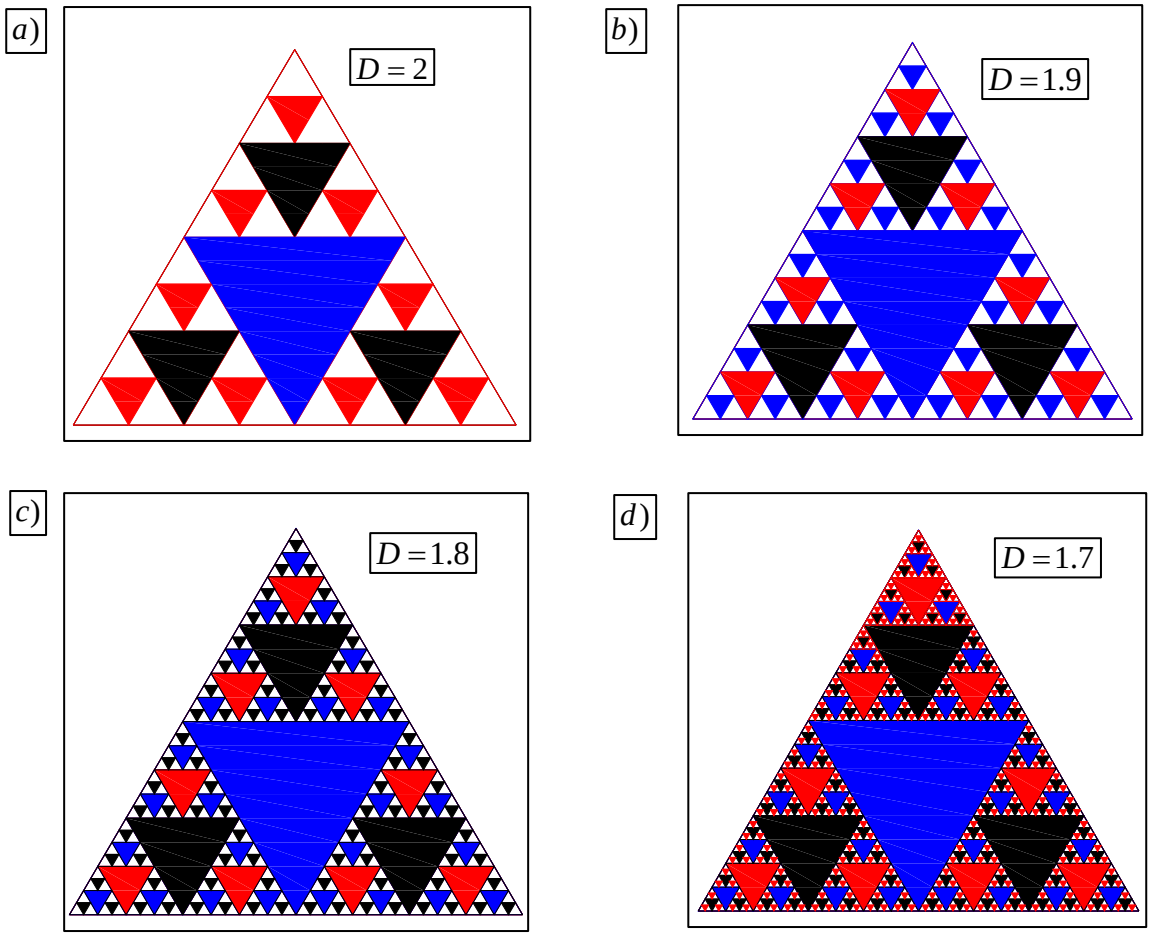

Figure 5-2 Levels of the Seirpinski Gasket (a) 3rd (b) 4th (c) 5th (d) 6th

At the third level of the gasket the fractal dimension has a value of 2 or 3 if applying it to a third dimension. The generated gasket does not have a number of different sized triangles. As the levels increase the generated gaskets have decreasing fractal dimensions. The sixth level of

the gasket has a fractal dimension of 1.7, or 2.7 in a three dimensional application. The last generated level of the gasket also has triangles of many different areas. In fact, as the levels increased and the fractal dimensions decreased the amount of different sized triangle also increased. This behavior acts like a uniform sample becoming well graded as the particles begin to fragment during compression.

5.4 SUMMARY

The fractal analysis showed the samples undergoing the tests with the applied vertical loads before the yield stress had low fragmentation fractal dimensions and were dominated by the larger particles. As the applied vertical load increased the fractal dimensions showed more fragmentation occurred within the samples. The sample from the 3 kN load had a dimension of 2.7, but the sample was not yet totally crushed as described by Turcotte(1997) as having a dimension of 2.5.

Another type of fractal was used to described how crushing occurs during compression. This was the Seirpinski Gasket. The gasket proved to be an adequate method to visually show what occurs inside a sample during fragmentation. Although six generations of the Seirpinski Gasket were generated, the fractal dimension did not match that of the level where infinite generations occurred.

6.0 CONCLUSIONS AND RECOMMENDATIONS

6.1 CONCLUSIONS

The main objective of this research was to try to visually see how crushing occurs in a weak granular material. It was shown that chick peas are an adequate material to use to model a weak granular material. The chick peas are not only large enough to be seen by the naked eye, but they also are weak enough standard laboratory equipment can be used on them. The main laboratory test used for the research was a uniaxial confined compression test. An initial test was run to a specific applied vertical load and from that load a series of other applied vertical loads was chosen. The initial test showed the sample underwent a substantial amount of deformation and severe particle breakage. The uniaxial confined compression tests run using the chosen loads showed the chick peas experienced a substantial amount of fragmentation. As the vertical load increased the number of crushed particles also increased. A sieve analysis showed the chick peas tended more toward the behavior of a well graded material as the applied vertical loads increased. The effective grain size for the samples decreased dramatically as the load increased as well as the permeability.

As mentioned one of the main objective of the research was to visually see the evolution of crushing. Both an internal and external evaluation was done. The external evaluation showed the chick peas first experienced particle breakage in the region of the sample closest to the

piston, but as the test went on all regions of the sample experienced particle breakage. The internal investigation showed the top region of the sample and the bottom region of the sample had different void ratios. The internal investigation also showed the breakage was not uniform throughout the sample at that particular applied vertical load.

A fractal analysis was also completed on the samples using both the Fragmentation Fractal Dimension as explained by Tyler and Wheatcraft and a Seirpinski Gasket. The Fragmentation Fractal Dimension analysis showed the samples from the tests where the applied vertical load was less that the yield stress were still dominated by the larger particles and underwent very little fragmentation. As the applied vertical load increased, so did the dimension and amount of fragmentation. Even though the sample from the highest applied load appeared to be undergo a large amount of crushing and had a high fractal dimension, it was not totally crushed. It was shown the Seirpinski Gasket can be an effective way to model the evolution of crushing in a weak granular material.

6.2 RECOMMENDATIONS FOR FUTURE RESEARCH

The results of this research prove chick peas can be used to model a granular material. It is recommended the chick peas continue to be used in trying to see the evolution of crushing in different ways than shown here. An example of a way to utilize the chick peas would be to use them to see how a weak granular material is affected by pile driving. They can be used to see how different shaped pile tips affect the breakage of the material surrounding the piles. The chick peas could also be used to study breakage in both dynamic and cyclic loading cases.

APPENDIX A

UNIAXIAL CONFINED COMPRESSION TESTS

Table A-1 Calculation for the Void Ratio Versus the Log of stress graph

Cyl. Area=	19.63495408	cm^2
Cyl. Area=	0.001963495	m^2
Gs=	1.399	
Mass=	108.6	g

Load (kN)= 0.003(reading)+0.0189*

Gauge Reading	Load (kN)	σ kPa	Vs (cm^3)	h of sample (cm)	e	lnσ kPa
0	0.02	9.63	77.63	9.80	1.48	2.26
100	0.32	162.41	77.63	9.60	1.43	5.09
200	0.62	315.20	77.63	9.55	1.42	5.75
300	0.92	467.99	77.63	9.25	1.34	6.15
400	1.22	620.78	77.63	8.30	1.10	6.43
500	1.52	773.57	77.63	7.85	0.99	6.65
600	1.82	926.36	77.63	7.55	0.91	6.83
700	2.12	1079.15	77.63	7.30	0.85	6.98
800	2.42	1231.94	77.63	6.95	0.76	7.12
900	2.72	1384.72	77.63	6.75	0.71	7.23
1000	3.02	1537.51	77.63	6.55	0.66	7.34

Photographs from the Applied Vertical Load of 0.5 kN

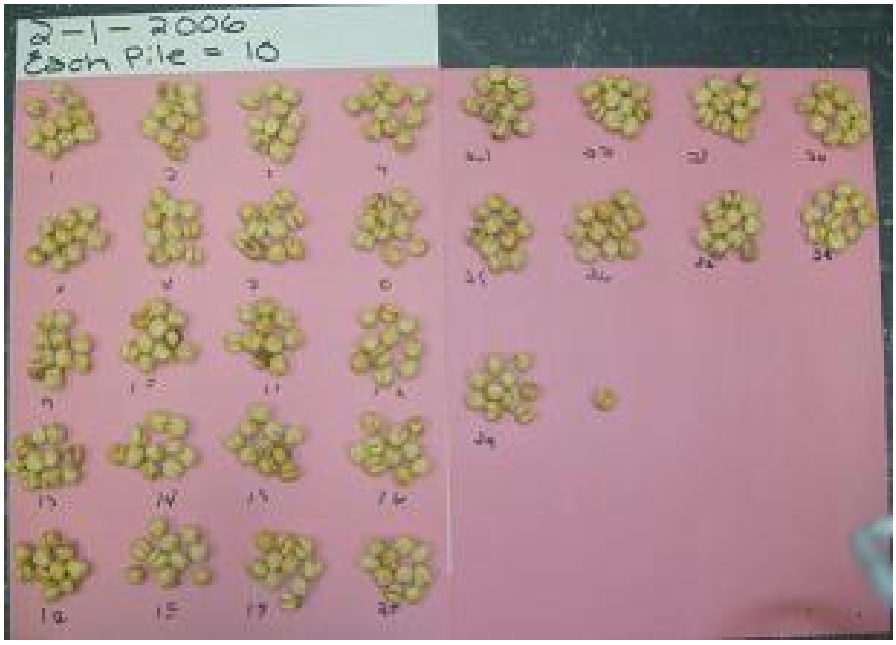

Number of chick peas before the test

Number of chick peas after the test

Sample in the machine before the test

Sample in the machine after the test

Top of the sample before the test

Top of sample after the test

Side of sample before test

Side of sample after the test

All of sample fell out of the cylinder

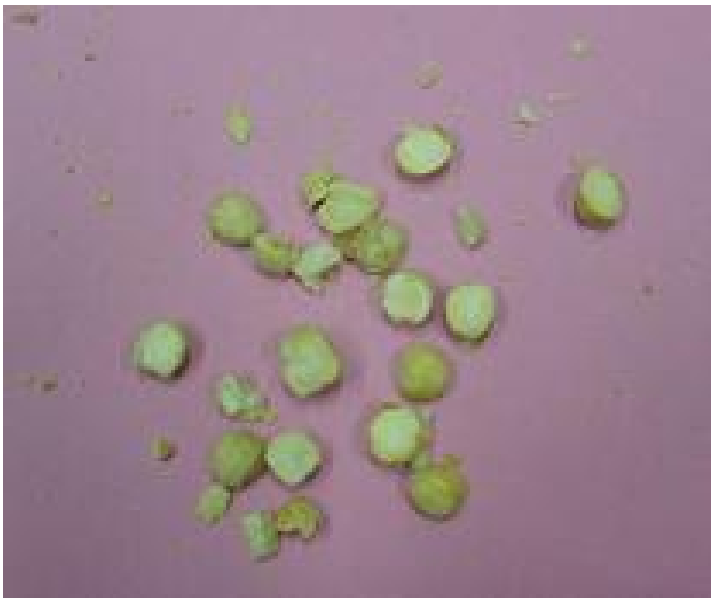

Crushed chick peas

Photographs from the Applied Vertical Load of 0.75 kN

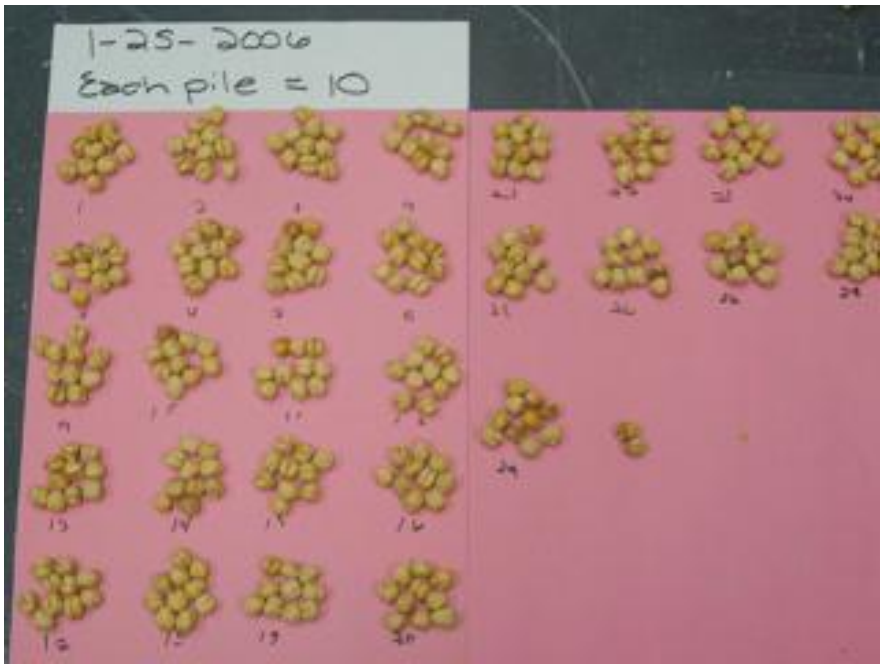

Number of chick peas before the test

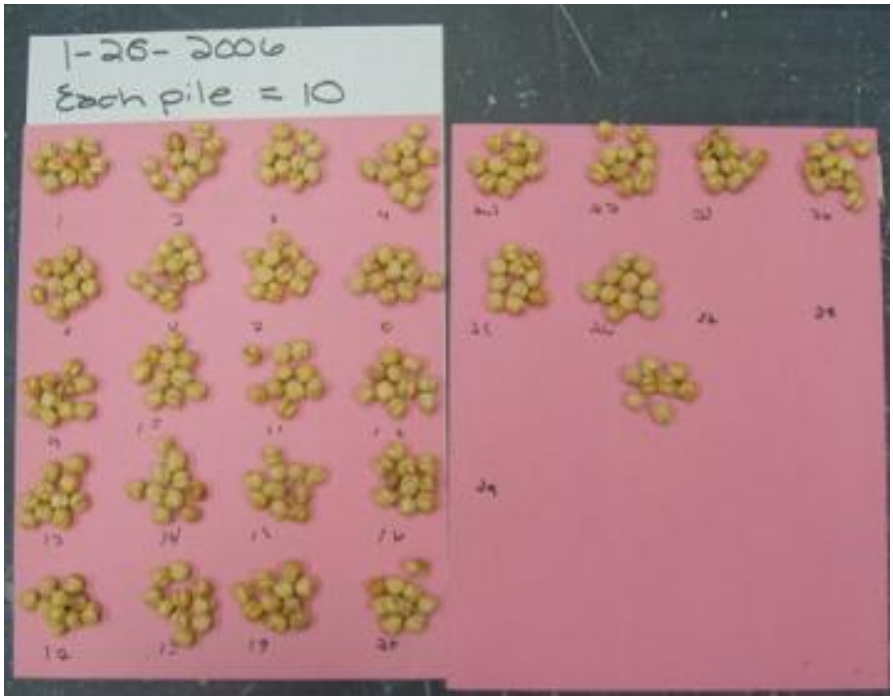

Number of chick peas after the test

Sample in the machine before the test

Sample in the machine after the test

Top of the sample before the test

Top of sample after the test

Side of sample before test

Side of sample after the test

All of sample fell out of the cylinder

Crushed chick peas

Photographs from the Applied Vertical Load of 1.5 kN

Number of chick peas before the test

Number of chick peas after the test

Sample in the machine before the test

Sample in the machine after the test

Top of the sample before the test

Top of sample after the test

Side of sample before test

Side of sample after the test

Middle of sample after test

A chunk of the sample remained in the cylinder

Crushed chick peas

Photographs from the Applied Vertical Load of 1.75 kN

Number of chick peas before the test

Number of intact chick peas after the test

Sample in the machine after the test

Sample in the machine after the test

Top of the sample before the test

Top of sample after the test

Side of sample after test

Side of sample after the test

The entire sample remained in the cylinder

Crushed chick peas

Photographs from the Applied Vertical Load of 3 kN

Number of intact chick peas

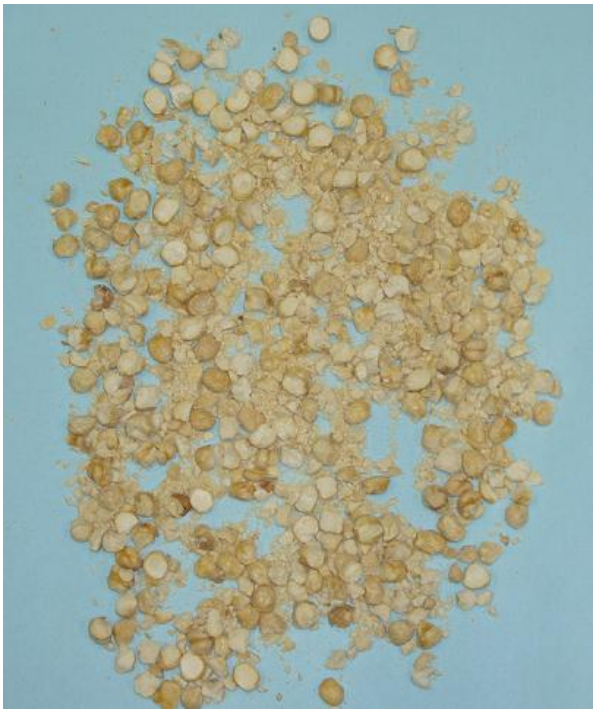

Number of crushed chick peas

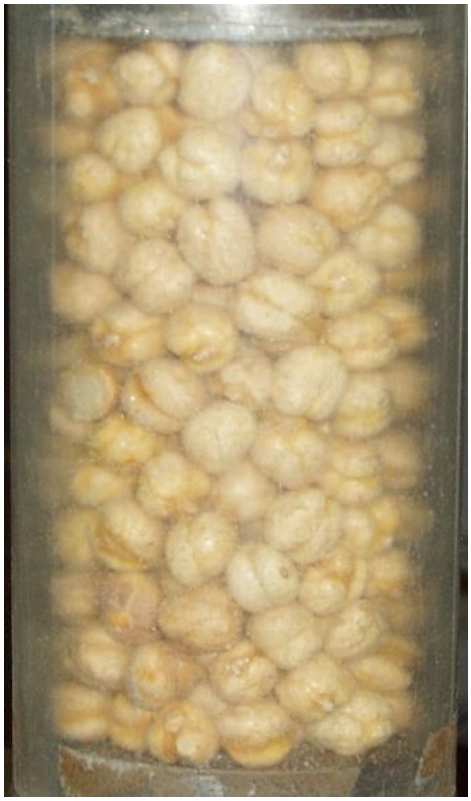

Sample in before the test

Sample in the machine after the test

APPENDIX B

SIEVE ANALYSIS

Table B-1 Sample Calculation of a PSD Plot

Sieve Analysis for 107.5 kN

Total Mass= 108.5 g

Sieve	Sieve Diameter(mm)	Wt Ce Ces Retained(g)	% Retained	Cumulative % Retained	% Finer
-	12.7	0	0	0	100
-	6.35	89.95	82.9338	82.93380048	17.0662
4	4.76	5.68	5.2369537	88.1707542	11.829246
10	2	6.77	6.2419325	94.4126867	5.5873133
20	0.841	2.38	2.1943574	96.60704407	3.3929559
40	0.42	0.88	0.811359	97.4184031	2.5815969
pan	-	2.8	2.5815969	100	0

Photographs from the Applied Vertical Load of 0.5 kN

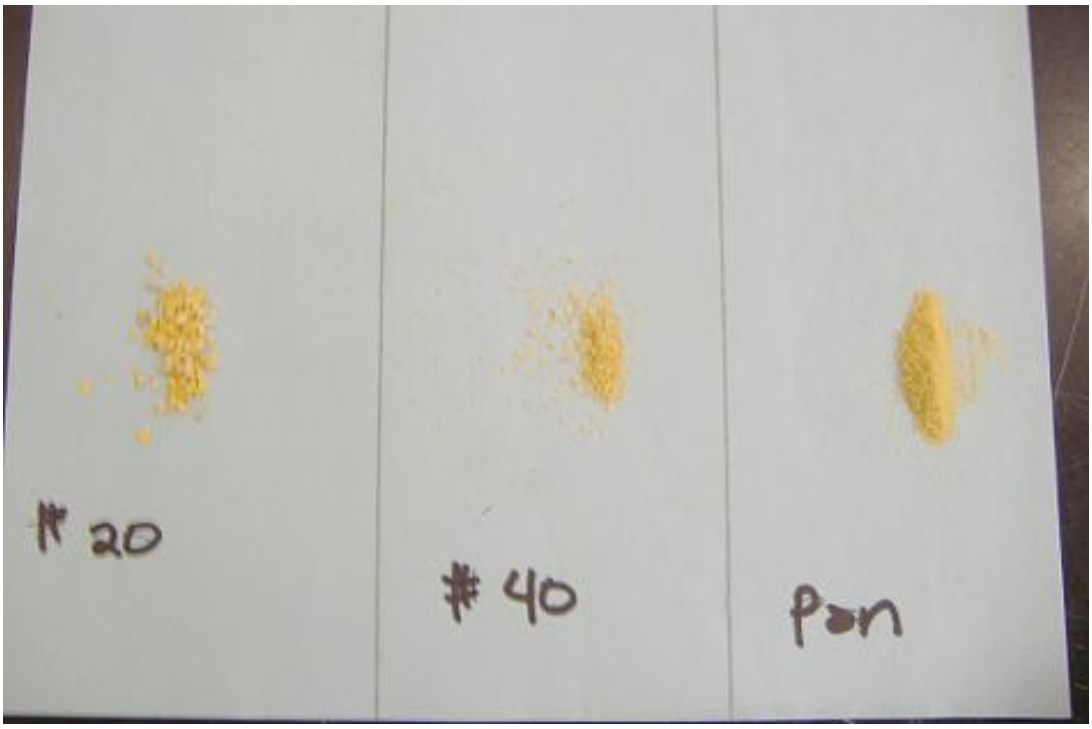

Photographs from the Applied Vertical Load of 0.75 kN

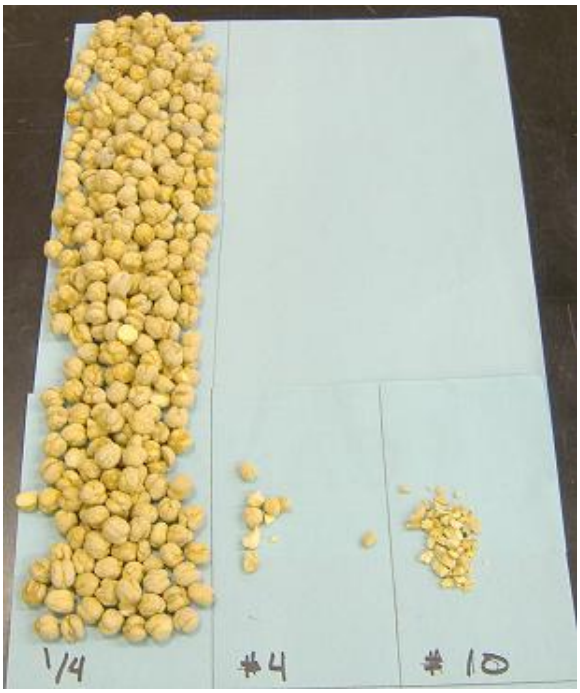

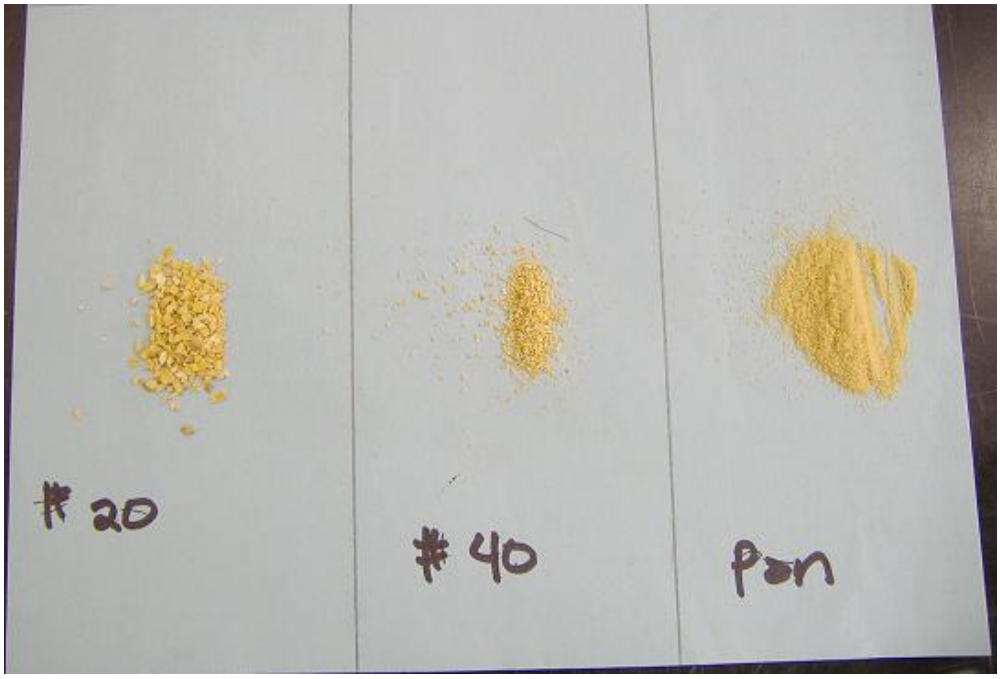

Photographs from the Applied Vertical Load of 1.5 kN

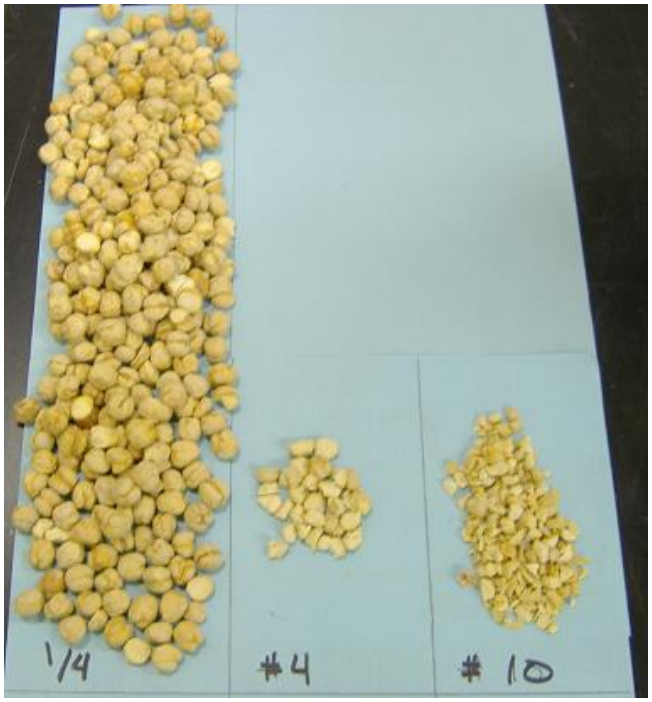

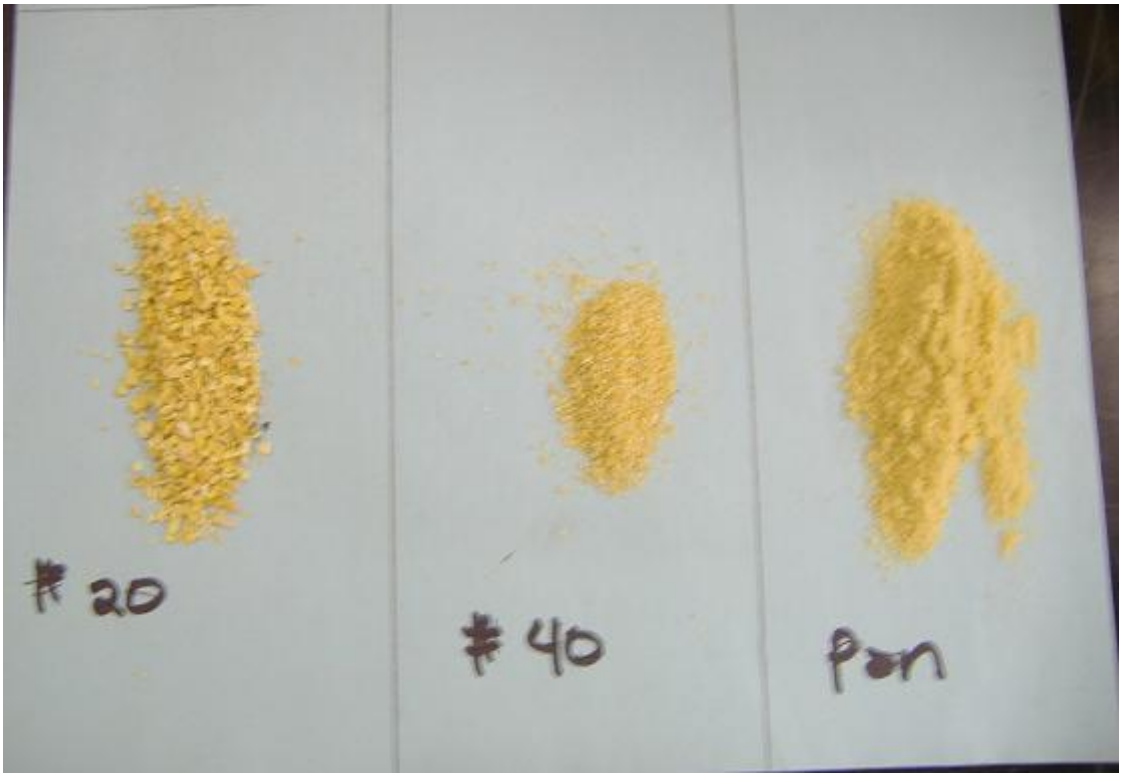

Photographs from the Applied Vertical Load of 1.75 kN

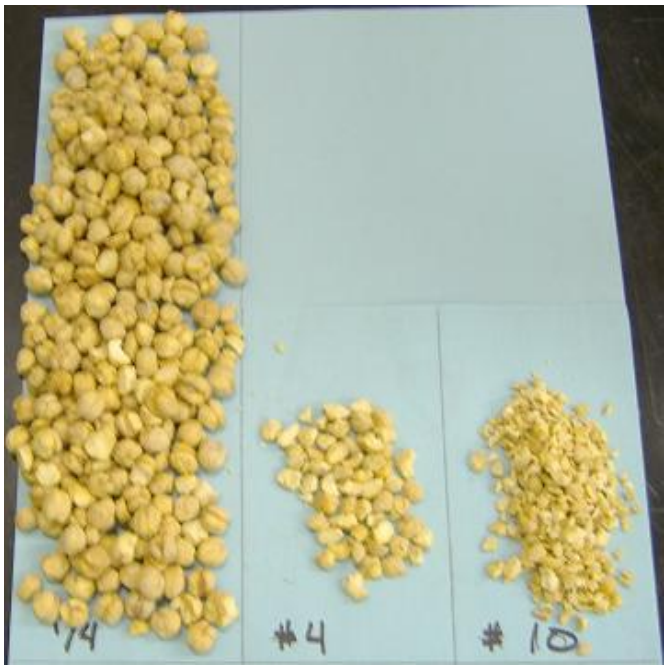

Photographs from the Applied Vertical Load of 3 kN

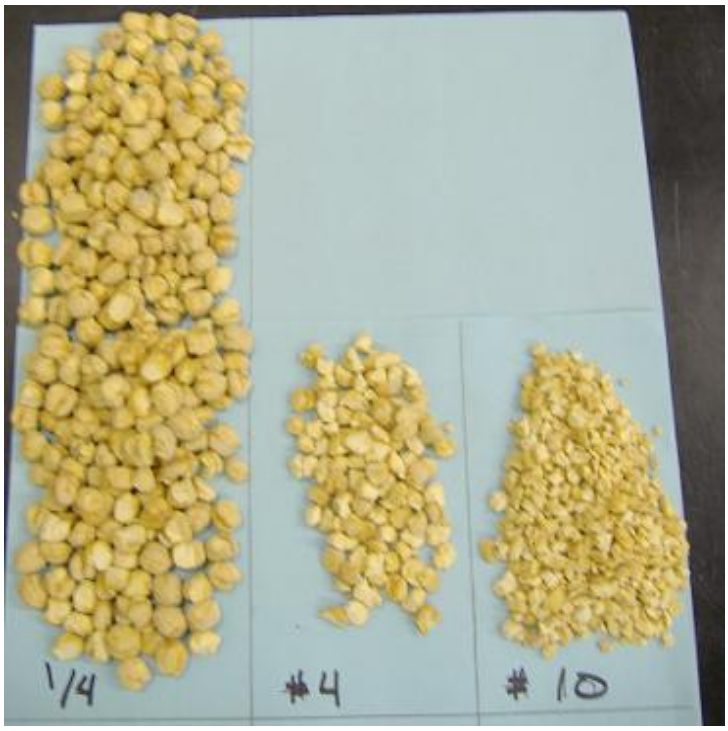

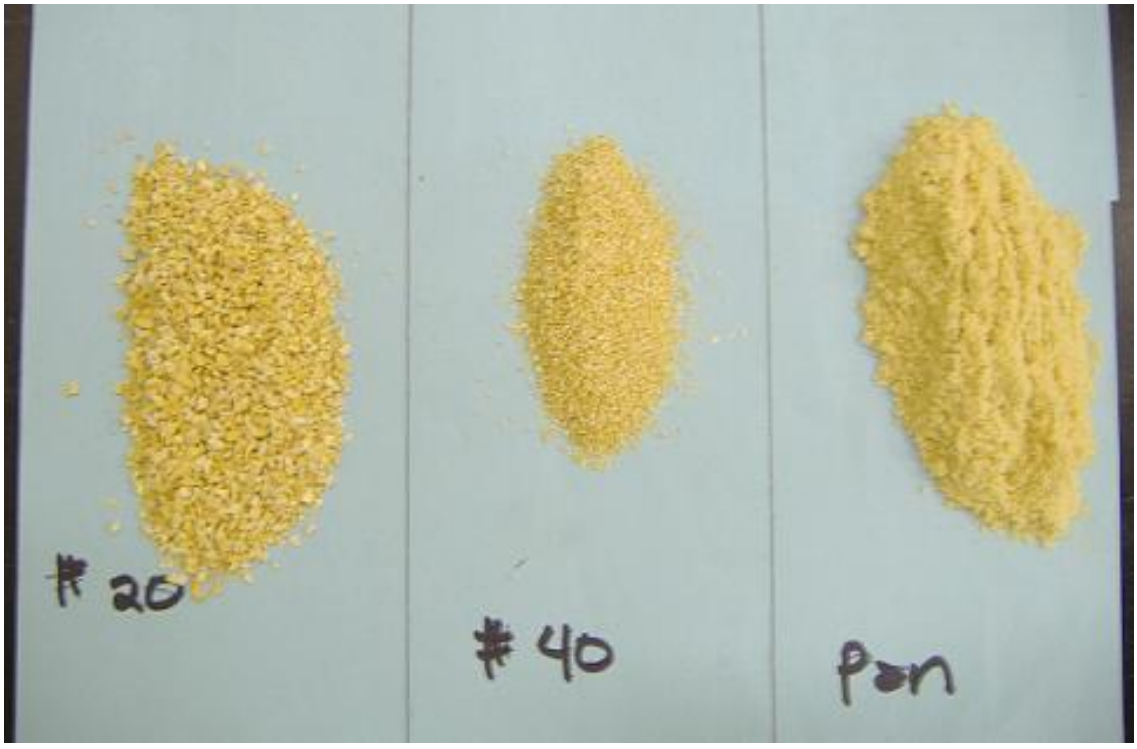

APPENDIX C

FRACTAL ANALYSIS

Table C-1 Sample of Fragmentation Fractal Dimension Calculation

Sieve	Sieve Diameter(mm)	Wt Ce Ces Retained(g)	% Retained	Cumulative % Retained	% Finer
-	12.7	0	0	0	100
-	6.35	89.95	82.9338	82.93380048	17.0662
4	4.76	5.68	5.2369537	88.1707542	11.829246
10	2	6.77	6.2419325	94.4126867	5.5873133
20	0.841	2.38	2.1943574	96.60704407	3.3929559
40	0.42	0.88	0.811359	97.4184031	2.5815969
pan	-	2.8	2.5815969	100	0

Sieve	Sieve Diameter(mm)	Wt Ce Ces Retained(g)	r/r_L	$M(R<r)/M_T$
-	12.7	0	1.00	1.00
-	6.35	89.95	0.50	0.17
4	4.76	5.68	0.37	0.12
10	2	6.77	0.16	0.06
20	0.841	2.38	0.07	0.03
40	0.42	0.88	0.03	0.03
pan	-	2.8	3-	0.97
			Df=	2.03

#	Area
Original	173.2051
1	43.3013
2	10.8253
3	2.7063
4	0.6766
5	0.1691
6	0.0423

a	A>a
0.0423	121
0.1691	40
0.6766	13
2.7063	4
10.8253	1

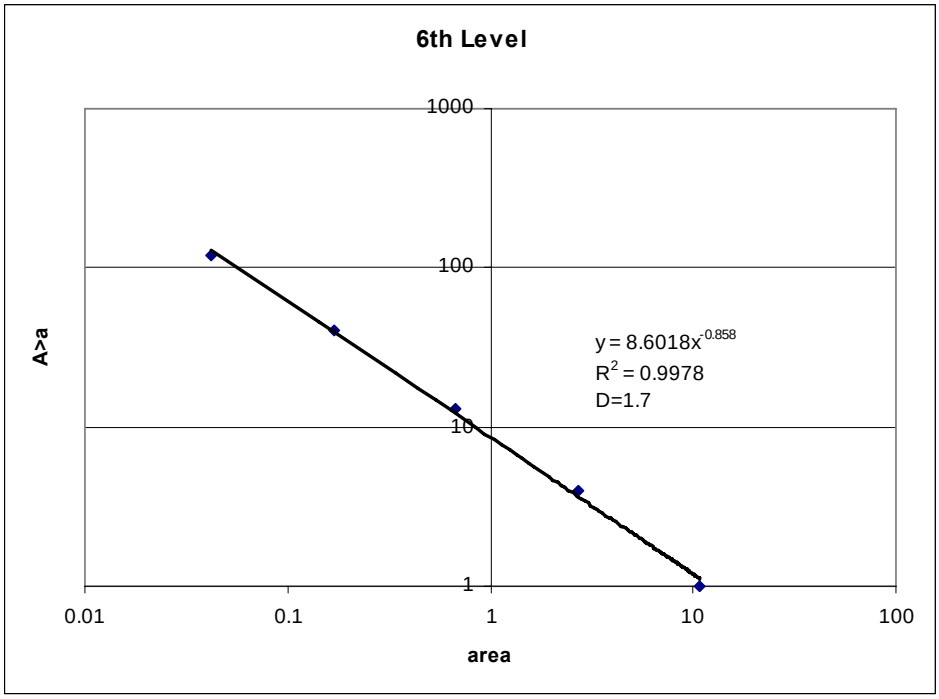

Figure C-1 Example calculation of the Seirpinski Gasket Fractal Dimension

BIBLIOGRAPHY

Bolton., M.D., *"The Strength and Dilatancy of Sands."* Geotechnique. 36.1 (1986): 65-78.

Chik, Zamri (2004) . "The Effect of Fragmentation on the Engineering Properties of Granular Materials: Laboratory and Fractal Analysis." Ph.D.Thesis, Department of Civil and Environmental Engineering, University of Pittsburgh.

Das, Braja M. Principles of Geotechnical Engineering. 5th ed. Pacific Cole: Brooks/Cole, 2002.

Feda, Jaroslav. "Notes on the effect of grain crushing on the granular soil behavior." Engineering Geology 63 (2002): 93-98.

Feder, Jans. Fractals. New York: Plenum Press, 1988.

Hagerty, M.M., D.R. Hite, C.R. Ullrich, and D.J. Hagerty. "One-Dimensional High-Pressure Compression of Granular Media." Journal of Geotechnical Engineering. 119.1 (1993): 1-18.

Hammer, Kevin (2005). "Analysis of Granular Materials in Pennsylvania Highways." Master's Thesis. Department of Civil and Environmental Engineering, University of Pittsburgh, .

Hyslip, James P., and Luis E. Vallejo. "Fractal analysis of the roughness and size distribution of granular materials." Engineering Geology 48 (1997): 231-244.

Lewis, Karl H., Luis F. Rojas-Gonzalez, and Carl Francisco Henderson. Soil Testing Manual. Pittsburgh: University of Pittsburgh, 1995.

Lobo-Guerrero, Sebastian (2005). "Evaluation of Crushing in granular Materials using the Discrete Element Method and Fractal Theory." Ph.D. Thesis, Department of Civil and Environmental Engineering, University of Pittsburgh,.

Lobo-Guerrero, Sebastian, Luis E. Vallejo, and Luis F. Vesga (2006) "Visualization of Crushing Evolution in Granular Materials Under Compression Using DEM." ASCE's International Journal of Geomechanics, Vol 6, No. 6, pp. 435-440

Lade, Poul V., Jerry A. Yamamuro, and Paul A. Bopp. “Significance of Particle Crushing in Granular Material.” Journal of Geotechnical Engineering. 122.4 (1996): 309-316.

Lee, Kenneth L., and Iraj Farhoomand. “Compressibility and Crushing of Granular Soil in Anisotropic Triaxial Compression.” Canadian Geotechnical Journal 4.1 (1967): 66-86.

Mandelbrot, Benoit B. The Fractal Geometry of Nature. San Francisco: W.H. Freeman and Company, 1982.

McDowell, G.R., and M.D. Bolton. ”On the micromechanics of crushable aggregates.” Geotechnique 48.5 (1998): 667-679.

McDowell, G.R., M.D. Bolton, and D. Robertson. “The Fractal Crushing of Granular Materials.” J. Mech. Phys. Solids 44.12 (1996): 2079-2102.

McDowell, G.R., and A. Humphreys. “Yielding of granular materials.” Granular Matter 4 (2002): 1-8.

McDowell, G.R., and J.J. Khan. “Creep of granular materials.” Granular Matter 5 (2003): 115-120.

Murff, James D. “Pile Capacity in Calcareous Sands: State of the Art.” Journal of Geotechnical Engineering 113.5 (1987): 490-507.

Turcotte, Donald L. Fractals and Chaos in Geology and Geophysics . 2nd ed. Cambridge: Cambridge University Press, 1997.

Tsoungui, Oliver, Denis Vallet, and Jean-Claude Charmet. ”Numerical model of crushing of grains inside two-dimensional granular materials.” Powder Technology 105 (1999): 190-198.

Tyler, S.W., and S.W. Wheatcraft. “Fractal scaling of soil particle-size distribution analysis and limitations.” Soil Sci. Soc. Am. J. 56.2 (1992): 47-67.

Vallejo, Luis E., Sebastian Lobo-Guerrero, and Zamri Chik (2005). “A Network of Fractal Force Chains and Their Effect in Granular Materials under Compression.” In; Fractals in Engineering, Levy-Vehel, J., and Lutton, E. (Editors). Springer, pp. 67-80.

Yasufuku, N., and A.F.L. Hyde. “Pile end-bearing capacity in crushable sands.” Geotechnique. 45.4 (1995): 663-676.